Edinburgh 96/31
CPT-97/P.3459
UG-DFM-1/97
SHEP 97/14
hep-lat/9709028

First Lattice Study of Semileptonic Decays of Λ_b and Ξ_b Baryons.

UKQCD Collaboration

K.C. Bowler[1], R.D. Kenway[1], L. Lellouch[2], J. Nieves[3], O. Oliveira[1] *, D.G. Richards[1], C.T. Sachrajda[4], N. Stella[4] and P. Ueberholz[1] †

[1]Department of Physics & Astronomy, The University of Edinburgh, Edinburgh EH9 3JZ, UK

[2]Centre de Physique Théorique‡, CNRS Luminy, Case 907 F-13288 Marseille Cedex 9, France

[3]Departamento de Fisica Moderna, Avenida Fuentenueva, 18071 Granada, Spain

[4]Department of Physics and Astronomy, University of Southampton, Highfield, Southampton SO17 1BJ, UK

*Present address: Departamente de Fisica, Universidade de Coimbra, 3000 Coimbra, Portugal

†Present address: Department of Physics, University of Wuppertal, Wuppertal D-42097, Germany

‡Unité Propre de Recherche 7061

Abstract

We present the results of the first lattice study of semileptonic decays of baryons containing a b-quark. Predictions for the decay distributions are given and the Isgur-Wise functions for heavy baryons are computed, for values of the velocity transfer up to about $\omega = 1.2$. The computations are performed on a $24^3 \times 48$ lattice at $\beta = 6.2$ using the Sheikholeslami-Wohlert action in the quenched approximation.

PACS Numbers: 14.20.Mr, 14.20.Lq, 13.30.Ce, 12.38.Gc, 12.39.Hg
Key-Words: Bottom Baryons, Charmed Baryons, Semileptonic Decays, Lattice QCD Calculation, Heavy Quark Effective Theory.

1 Introduction

The discovery of the Λ_b baryon at LEP [1] and the observation of its semileptonic decay [2] makes a study of the weak interactions of heavy baryons on the lattice timely. A knowledge of the strong interaction effects in semileptonic decays is necessary for the determination of the V_{cb} element of the CKM matrix from the experimentally measured rates and distributions. Up to now $|V_{cb}|$ has been measured from the inclusive and exclusive decays of heavy mesons.

In this paper we present the results of the first non-perturbative computation of the semileptonic decays of heavy baryons performed using lattice QCD, encouraged by our previous results on the spectroscopy [3]. The main purpose of this first study is to establish whether such a calculation is feasible, and to identify the principal sources of systematic uncertainties and statistical fluctuations. Nevertheless, in spite of the exploratory character of this investigation, we are able to determine the main features exhibited by the six form factors which enter in the decay amplitude for the processes $\Lambda_b \to \Lambda_c + l\bar{\nu}$ and $\Xi_b \to \Xi_c + l\bar{\nu}$, and hence to extract a considerable amount of phenomenologically interesting information.

Using Heavy Quark Symmetry it is possible to relate the six form factors to a unique baryonic Isgur-Wise function, $\xi(\omega)$ [4], where $\omega = v \cdot v'$, and v and v' are the four-velocities of the initial and final state baryons. We compute $\xi(\omega)$, and by studying the dependence of the form factors on the mass (or masses) of the heavy quark, m_Q, we are able to use Heavy Quark Effective Theory (HQET) to give an estimate of the $\mathcal{O}(1/m_Q)$ corrections to the infinite-mass results (for a review and references to the original literature see Ref. [5]). The dependence of the Isgur-Wise function on the masses of the light quarks is more uncertain because of our limited data. In particular, we performed the simulations at two values of the light-quark mass (a little larger and a little smaller than that of the strange quark). Although the results for these masses are very encouraging, a significant uncertainty is introduced when the results are extrapolated, as a function of the masses of the light quarks, to the chiral limit. We present the results for the Isgur-Wise function for massless light quarks (relevant for the decay $\Lambda_b \to \Lambda_c + l\bar{\nu}$), as well as for the case in which one light quark is massless and other is the strange quark, relevant for the process $\Xi_b \to \Xi_c + l\bar{\nu}$. One of the main goals of a future simulation will be to determine, in detail, the dependence of $\xi(\omega)$ on the masses of the light quarks, and hence to reduce the uncertainty due to the extrapolation of the results to physical masses.

We obtain for the decay rate integrated over the range $\omega \in [1, 1.2]$

$$\begin{aligned} \int_1^{1.2} d\omega \, \frac{d\Gamma}{d\omega}(\Lambda_b \to \Lambda_c + l\bar{\nu}) &= 1.4 \; {}^{+5}_{-4} \; |V_{cb}|^2 \, 10^{13} \, s^{-1} \\ \int_1^{1.2} d\omega \, \frac{d\Gamma}{d\omega}(\Xi_b \to \Xi_c + l\bar{\nu}) &= 1.6 \; {}^{+4}_{-5} \; |V_{cb}|^2 \, 10^{13} \, s^{-1}. \end{aligned} \tag{1}$$

This range of ω corresponds to that for which we have the most reliable results. We also obtain the slopes of the differential-decay-rate form factors which are to be compared to the slopes obtained by performing fits to experimental results for $d\Gamma/d\omega$ versus ω, for ω near 1, when such results become available. We find:

$$\rho^2_{\mathcal{B}} = 1.1 \pm 1.0 \tag{2}$$

for $\Lambda_b \to \Lambda_c \ell \bar{\nu}$ decays and

$$\rho^2_{\mathcal{B}} = 1.4 \pm 0.8 \tag{3}$$

for $\Xi_b \to \Xi_c \ell \bar{\nu}$ decays. A more detailed discussion is presented in Section 6.2.

The plan of the paper is the following: in Section 2 we recapitulate the theoretical framework for the definition of the baryonic Isgur-Wise function. Section 3 gives details of the simulation and Section 4 presents the results of the numerical analysis of both two- and three-point functions. We study the dependence of the Isgur-Wise function on the velocity transfer and on the masses of the heavy and light quarks in Section 5. In Section 6, we consider the phenomenological implications of our results for the baryonic Isgur-Wise function and give estimates of differential and partially-integrated decay rates. The main body of the paper is accompanied by three appendices where we lay out some lengthy parts of the calculation and of the analysis.

For the reader who is not interested in the details of the computation we have attempted to write Sections 2 (theoretical framework) and 6 (results and implications for phenomenology) in a self-contained way.

2 Theoretical background

In this section we outline the theoretical framework needed to study the semileptonic decays of Λ_b and Ξ_b baryons. The two baryons differ in their light flavour content, but are identical in all other quantum numbers and, in particular, they can be described in the same manner within the framework of HQET. For simplicity we will only consider the Λ_b decay.

The non-perturbative strong interaction effects in the exclusive semileptonic decay of the Λ_b are contained in the matrix elements of the $V-A$ weak current, $J_\mu = \bar{c}\gamma_\mu(1-\gamma_5)b$, which can be written in terms of six invariant form factors, f_i, g_i with $i = 1, 2, 3$, as follows:

$$\begin{aligned}\langle \Lambda_c^{(s)}(p')|J_\mu|\Lambda_b^{(r)}(p)\rangle = \bar{u}_c^{(s)}(p') \quad & [\gamma_\mu(f_1 - \gamma_5 g_1) + i\sigma_{\mu\nu}q^\nu(f_2 - \gamma_5 g_2) \\ & + iq_\mu(f_3 - \gamma_5 g_3)]\, u_b^{(r)}(p).\end{aligned} \tag{4}$$

In Eq. (4), the momenta and polarisations of the initial and final baryons have been explicitly indicated. The form factors are functions of q^2, where q is the

4-momentum transfer ($q = p' - p$). The decomposition above is convenient since, if the lepton masses are neglected, only the dominant form factors f_1 and g_1 contribute to the rate. Since both the quarks destroyed and created by J_μ are heavy, HQET provides a useful guide to the study of the form factors. In addition, the Λ_b baryon has a particularly simple structure in that it is composed of a heavy quark and light degrees of freedom with zero total angular momentum, so that Heavy Quark Symmetry has considerable predictive power. Expression (4) can be rewritten in terms of the velocity variables $v_\mu = p_\mu/M_{\Lambda_b}$ and $v'_\mu = p'_\mu/M_{\Lambda_c}$ using a different set of form factors, which are functions of the velocity transfer $\omega = v \cdot v'$:

$$\langle \Lambda_c^{(s)}(v')|\bar{c}\gamma_\mu(1-\gamma_5)b|\Lambda_b^{(r)}(v)\rangle = \\ \bar{u}_c^{(s)}(v')\left[\gamma_\mu(F_1 - \gamma_5 G_1) + v_\mu(F_2 - \gamma_5 G_2) + v'_\mu(F_3 - \gamma_5 G_3)\right] u_b^{(r)}(v). \qquad (5)$$

In principle, we do not need to use HQET at all but can evaluate the matrix elements in Eq. (4) directly. However, as the inverse lattice spacing in our calculation is about 2.9 GeV, we cannot use the physical b-quark mass in our computation. Instead, we evaluate the matrix element in Eq. (4) for a variety of "b" and "c" quark masses in the region of the physical charm quark mass, and extrapolate the results to the physical values. HQET provides us with the theoretical framework to perform this extrapolation. The hadronic form factors F_i, G_i can be expanded in inverse powers of the heavy-quark masses; the non-perturbative QCD effects in the coefficients of this expansion are universal, mass-independent functions of the velocity transfer. This is achieved by constructing an operator product expansion of the weak currents. The analysis at leading order [4] establishes the important result that all the baryonic form factors are described by a single universal function called the (baryonic) Isgur-Wise function, $\xi(\omega, \mu)$, [1]

$$\langle \Lambda_c^{(s)}(v')|\bar{c}\gamma_\nu(1-\gamma_5)b|\Lambda_b^{(r)}(v)\rangle = \xi(\omega,\mu)\bar{u}_c^{(s)}(v')\gamma_\nu(1-\gamma_5)u_b^{(r)}(v), \qquad (6)$$

which is normalized to the identity at $\omega = 1$ and where μ is the scale at which ξ is renormalized. The relation between the six form factors and the renormalized Isgur-Wise function is given at leading order by the expressions [5, 6]

$$F_i(\omega) = \hat{C}_i(\omega)\xi^{\rm ren}(\omega), \qquad G_i(\omega) = \hat{C}_i^5(\omega)\xi^{\rm ren}(\omega), \qquad (7)$$

where the scale dependence of the Isgur-Wise function $\xi(\omega, \mu)$ is reabsorbed into the definition of the short distance coefficients $\hat{C}_i^{(5)}(\omega)$. The coefficient functions $\hat{C}_i^{(5)}$ are known up to order $\alpha_s^2(z \log z)^n$, where $z = m_c/m_b$ is the ratio of the

[1] We draw the reader's attention to the fact that the Isgur-Wise function which describes baryonic weak matrix elements is different from that entering in mesonic transitions. For simplicity we shall use the name Isgur-Wise function to refer to the baryonic one, whenever this does not lead to ambiguities.

heavy-quark masses and $n = 0, 1, 2$. The perturbative expansion of $\hat{C}_1$ and $\hat{C}_1^5$ is of the form

$$\hat{C}_1^{(5)} = 1 + \delta_1^{(5)}(\omega)\alpha_s + ... \tag{8}$$

whereas the expansion of $\hat{C}_{2,3}^{(5)}$ starts at $\mathcal{O}(\alpha_s)$. The perturbative corrections are rather small since the coefficients of α_s are typically of order 1, for our range of masses and values of ω, so that $\hat{C}_{2,3}^{(5)}$ are much smaller than $\hat{C}_1^{(5)}$ ($\hat{C}_{2,3}^{(5)} \sim 0.2\,\hat{C}_1^{(5)}$).

We also attempt below to obtain some information on the $1/m_Q$ corrections to the form factors. In order to include these corrections it is convenient to define a new function (see Ref. [5])

$$\hat{\xi}_{QQ'}(\omega) = \xi^{\rm ren} + \Big(\frac{\bar{\Lambda}}{2m_Q} + \frac{\bar{\Lambda}}{2m'_Q}\Big)\left[2\chi^{\rm ren}(\omega) + \frac{\omega-1}{\omega+1}\xi^{\rm ren}(\omega)\right] \tag{9}$$

which is also scale-independent and normalized at zero recoil, since the function $\chi(\omega)$, arising from the higher-dimension operators in the HQET Lagrangian, vanishes at $\omega = 1$.

$\bar{\Lambda}$ in Eq. (9) is the binding energy of the heavy quark in the corresponding Λ-baryon,

$$\bar{\Lambda} = M_{\Lambda_b} - m_b = M_{\Lambda_c} - m_c \ , \tag{10}$$

up to $1/m_Q$ corrections. The quark masses in Eq. (10) are generally taken to be pole masses, which contain renormalon ambiguities of $\mathcal{O}(\Lambda_{QCD})$. For the form factors, the ambiguities due to $\bar{\Lambda}$ are cancelled by those arising from the higher-order terms in the perturbative series for the coefficients $\hat{C}_i^{(5)}(\omega)$. In practice, we only know the coefficients $\hat{C}_i^{(5)}(\omega)$ up to one-loop order, and we implicitly assume that $\bar{\Lambda}$ is obtained from some physical quantity with a similar precision. As we note in Section 6, some of the freedom of what to assign to the coefficients and what to the power corrections cancels in the prediction for the physical form factors obtained from those calculated on the lattice.

$\hat{\xi}_{QQ'}$ is not a universal function and its dependence on the flavour of the heavy quarks must be studied in detail (see Section 5.1). The relation between the new function $\hat{\xi}_{QQ'}(\omega)$ and the form factors is given by

$$\begin{aligned} F_i(\omega) &= N_i(\omega)\hat{\xi}_{QQ'}(\omega) + \mathcal{O}\left(1/m^2_{Q^{(\prime)}}\right), \\ G_i(\omega) &= N_i^5(\omega)\hat{\xi}_{QQ'}(\omega) + \mathcal{O}\left(1/m^2_{Q^{(\prime)}}\right), \end{aligned} \tag{11}$$

where the coefficients $N_i^{(5)}$ contain both radiative and $1/m_Q$ corrections. The exact expressions are [5]

$$N_1(\omega) = \hat{C}_1(\bar{\omega})\left[1 + \frac{2}{\omega+1}\Big(\frac{\bar{\Lambda}}{2m_Q} + \frac{\bar{\Lambda}}{2m_{Q'}}\Big)\right],$$

$$
\begin{aligned}
N_2(\omega) &= \hat{C}_2(\bar{\omega})\left(1+\frac{2\omega}{\omega+1}\frac{\bar{\Lambda}}{2m_Q}\right)-\left[\hat{C}_1(\bar{\omega})+\hat{C}_3(\bar{\omega})\right]\frac{2}{\omega+1}\frac{\bar{\Lambda}}{2m_{Q'}}\,,\\
N_3(\omega) &= \hat{C}_3(\bar{\omega})\left(1+\frac{2\omega}{\omega+1}\frac{\bar{\Lambda}}{2m_{Q'}}\right)-\left[\hat{C}_1(\bar{\omega})+\hat{C}_2(\bar{\omega})\right]\frac{2}{\omega+1}\frac{\bar{\Lambda}}{2m_{Q}}\,,\\
N_1^5(\omega) &= \hat{C}_1^5(\bar{\omega})\,,\\
N_2^5(\omega) &= \hat{C}_2^5(\bar{\omega})\left(1+\frac{2}{\omega+1}\frac{\bar{\Lambda}}{2m_{Q'}}+\frac{\bar{\Lambda}}{m_Q}\right)\\
&- \left[\hat{C}_1^5(\bar{\omega})+\hat{C}_3^5(\bar{\omega})\right]\frac{2}{\omega+1}\frac{\bar{\Lambda}}{2m_{Q'}}\,,\\
N_3^5(\omega) &= \hat{C}_3^5(\bar{\omega})\left(1+\frac{2}{\omega+1}\frac{\bar{\Lambda}}{2m_{Q}}+\frac{\bar{\Lambda}}{m_{Q'}}\right)\\
&+ \left[\hat{C}_1^5(\bar{\omega})-\hat{C}_2^5(\bar{\omega})\right]\frac{2}{\omega+1}\frac{\bar{\Lambda}}{2m_{Q}}\,.
\end{aligned}
\tag{12}
$$

where the "velocity transfer of the free quark" $\bar{\omega}$ is given by

$$
\bar{\omega} = \omega + (\omega-1)\left(\frac{\bar{\Lambda}}{m_Q}+\frac{\bar{\Lambda}}{m_{Q'}}\right). \tag{13}
$$

At zero recoil, Luke's theorem [7] protects the quantities $\sum_i F_i(1)$ and $G_1(1)$ from $\mathcal{O}(1/m_Q)$ corrections:

$$
\begin{aligned}
\sum_i F_i(1) = \sum_i \hat{C}_i(1) + \mathcal{O}(1/m_Q^2) \quad &\to \quad \frac{\sum_i F_i(1)}{N_{\rm sum}(1)} = 1+\mathcal{O}(1/m_Q^2)\\
G_1(1) = \hat{C}_1^5(1) + \mathcal{O}(1/m_Q^2) \quad &\to \quad \frac{G_1(1)}{N_1^5(1)} = 1+\mathcal{O}(1/m_Q^2).
\end{aligned}
\tag{14}
$$

For degenerate quark masses, $m_Q = m_{Q'}$, the coefficient

$$
\begin{aligned}
N_{\rm sum}(\omega) = \sum_i N_i(\omega) = \hat{C}_1(\bar{\omega}) &+ \hat{C}_2(\bar{\omega})\left(1+\frac{2(\omega-1)}{\omega+1}\frac{\bar{\Lambda}}{2m_Q}\right)\\
&+ \hat{C}_3(\bar{\omega})\left(1+\frac{2(\omega-1)}{\omega+1}\frac{\bar{\Lambda}}{2m_{Q'}}\right),
\end{aligned}
\tag{15}
$$

equals one at zero recoil, as required by vector current conservation.

The coefficients (12) and (15) depend on the heavy-quark masses and on the value of the baryonic binding energy $\bar{\Lambda}$. Different choices for the definition and values of the quark masses to be used in these expressions lead to differences which are of $\mathcal{O}(\alpha_s^2)$ and $\mathcal{O}(1/m_Q^2)$, and hence are formally of the size of the terms we are neglecting. Moreover, we find that different choices of the quark mass lead to negligible differences in the form factors for F_1, $\sum_i F_i$ and G_1. This is not the

κ_Q	$M_P\, a$	$M_V\, a$	m_Q(GeV)
0.121	$0.874\ ^{+4}_{-3}$	$0.896\ ^{+5}_{-4}$	2.38
0.125	$0.773\ ^{+3}_{-3}$	$0.799\ ^{+4}_{-3}$	2.10
0.129	$0.665\ ^{+3}_{-3}$	$0.696\ ^{+4}_{-4}$	1.80
0.133	$0.547\ ^{+3}_{-3}$	$0.588\ ^{+4}_{-5}$	1.48

Table 1: *Values of the quark masses in physical units, for $a^{-1} = 2.9$ GeV and $\bar{\Lambda} = 200$ MeV, as obtained from the pseudoscalar and vector meson masses in lattice units. (κ_Q is the heavy quark's hopping parameter.)*

case for the form factors F_2, F_3 and G_2, G_3, however, for which the coefficient functions are zero at tree level and for which the $\mathcal{O}(1/m_Q)$ terms represent a major contribution. In these cases we take $m_Q = M_\Lambda - \bar{\Lambda}$, and $\bar{\Lambda}$ is obtained from a fit of the theoretical prediction for the form factors to the lattice results (see Section 5.3). In all other cases, where the results are insensitive to the choice of the quark mass, we take

$$m_Q = \frac{a^{-1}}{4}(3M_V + M_P) - 200 \text{ MeV} \tag{16}$$

where M_V and M_P are the masses of the vector and pseudoscalar heavy-light mesons, as measured very precisely from a previous simulation performed on the same set of configurations. 200 MeV is an estimate of the spin-averaged mesonic binding energy [8]. For the lattice spacing, as discussed in greater detail in Section 3, we take

$$a^{-1} = 2.9 \pm 0.2 \text{ GeV}. \tag{17}$$

The values of the quark masses obtained in this way are presented in Table 1, and the coefficients $N_i^{(5)}$ and $\hat{C}_i$ which are used in the rest of this paper are reported in Tables 2 and 3 for $\Lambda_{QCD} = 250$ MeV and $n_f = 0$ (as may be more appropriate for a quenched calculation).

Below, we will proceed as follows. Since N_1^5 and $N_{\rm sum}$ are close to unity and the form factors $G_1(\omega)$ and $\sum_i F_i(\omega)$ are insensitive to the value of $\bar{\Lambda}$, we can use the measured values of these form factors to determine the Isgur-Wise function reliably. For the individual vector form factors F_1, F_2 and F_3 (and similarly for G_2 and G_3) the situation is different since the $\mathcal{O}(1/m_Q)$ corrections are significant. From these form factors, using the Isgur-Wise function already obtained, we determine the $\bar{\Lambda}$ parameter. Finally we use the combined results to determine the form factors for the physical $b \to c$ decays.

$\kappa_Q \to \kappa_{Q'}$	ω	$\bar{\omega}$	$N_1^5(\omega) = \hat{C}_1^5(\bar{\omega})$	$\hat{C}_2(\bar{\omega})$	$\hat{C}_1(\bar{\omega})$	$N_{\rm sum}(\omega)$
$0.121 \to 0.121$	1.0	1.0	0.961	0.019	0.961	1.0
$0.121 \to 0.125$	1.0	1.0	0.965	0.024	0.965	1.01
$0.121 \to 0.129$	1.0	1.0	0.971	0.03	0.971	1.02
$0.121 \to 0.133$	1.0	1.0	0.98	0.04	0.98	1.04
$0.125 \to 0.121$	1.0	1.0	0.956	0.016	0.956	0.992
$0.125 \to 0.125$	1.0	1.0	0.959	0.02	0.959	1.0
$0.125 \to 0.129$	1.0	1.0	0.965	0.027	0.965	1.01
$0.125 \to 0.133$	1.0	1.0	0.973	0.037	0.973	1.03
$0.129 \to 0.121$	1.0	1.0	0.949	0.011	0.949	0.982
$0.129 \to 0.125$	1.0	1.0	0.952	0.016	0.952	0.989
$0.129 \to 0.129$	1.0	1.0	0.957	0.022	0.957	1.0
$0.129 \to 0.133$	1.0	1.0	0.964	0.031	0.964	1.02
$0.133 \to 0.121$	1.0	1.0	0.938	0.0044	0.938	0.967
$0.133 \to 0.125$	1.0	1.0	0.941	0.0086	0.941	0.973
$0.133 \to 0.129$	1.0	1.0	0.945	0.015	0.945	0.984
$0.133 \to 0.133$	1.0	1.0	0.952	0.024	0.952	1.0
$0.121 \to 0.121$	1.1	1.15	0.932	0.018	0.932	0.968
$0.121 \to 0.125$	1.1	1.15	0.937	0.022	0.937	0.977
$0.121 \to 0.129$	1.1	1.16	0.944	0.028	0.944	0.99
$0.121 \to 0.133$	1.1	1.17	0.955	0.037	0.955	1.01
$0.125 \to 0.121$	1.1	1.15	0.927	0.014	0.927	0.96
$0.125 \to 0.125$	1.1	1.16	0.931	0.018	0.931	0.969
$0.125 \to 0.129$	1.1	1.16	0.938	0.024	0.938	0.981
$0.125 \to 0.133$	1.1	1.17	0.948	0.033	0.948	1.0
$0.129 \to 0.121$	1.1	1.16	0.92	0.01	0.92	0.95
$0.129 \to 0.125$	1.1	1.16	0.924	0.014	0.924	0.958
$0.129 \to 0.129$	1.1	1.17	0.93	0.02	0.93	0.97
$0.129 \to 0.133$	1.1	1.17	0.94	0.028	0.94	0.99
$0.133 \to 0.121$	1.1	1.17	0.91	0.0039	0.91	0.935
$0.133 \to 0.125$	1.1	1.17	0.913	0.0077	0.913	0.943
$0.133 \to 0.129$	1.1	1.17	0.919	0.013	0.919	0.954
$0.133 \to 0.133$	1.1	1.18	0.929	0.021	0.929	0.973

Table 2: *Radiative and $\mathcal{O}(1/m_Q)$ correction factors for $\omega = 1.0$ and 1.1. (κ_Q and $\kappa_{Q'}$ are the initial and final heavy quark hopping parameters.)*

$\kappa_Q \to \kappa_{Q'}$	ω	$\bar{\omega}$	$N_1^5(\omega) = \hat{C}_1^5(\bar{\omega})$	$\hat{C}_2(\bar{\omega})$	$\hat{C}_1(\bar{\omega})$	$N_{\rm sum}(\omega)$
$0.121 \to 0.121$	1.2	1.3	0.904	0.016	0.904	0.937
$0.121 \to 0.125$	1.2	1.31	0.909	0.02	0.909	0.946
$0.121 \to 0.129$	1.2	1.32	0.917	0.025	0.917	0.96
$0.121 \to 0.133$	1.2	1.33	0.929	0.034	0.929	0.981
$0.125 \to 0.121$	1.2	1.31	0.898	0.013	0.898	0.929
$0.125 \to 0.125$	1.2	1.31	0.903	0.017	0.903	0.938
$0.125 \to 0.129$	1.2	1.32	0.911	0.022	0.911	0.951
$0.125 \to 0.133$	1.2	1.34	0.923	0.03	0.923	0.972
$0.129 \to 0.121$	1.2	1.32	0.891	0.0091	0.891	0.919
$0.129 \to 0.125$	1.2	1.32	0.896	0.013	0.896	0.928
$0.129 \to 0.129$	1.2	1.33	0.903	0.018	0.903	0.941
$0.129 \to 0.133$	1.2	1.35	0.915	0.026	0.915	0.961
$0.133 \to 0.121$	1.2	1.33	0.881	0.0034	0.881	0.905
$0.133 \to 0.125$	1.2	1.34	0.886	0.0069	0.886	0.913
$0.133 \to 0.129$	1.2	1.35	0.893	0.012	0.893	0.925
$0.133 \to 0.133$	1.2	1.36	0.904	0.019	0.904	0.945
$0.121 \to 0.121$	1.3	1.45	0.876	0.015	0.876	0.907
$0.121 \to 0.125$	1.3	1.46	0.882	0.018	0.882	0.916
$0.121 \to 0.129$	1.3	1.48	0.89	0.023	0.89	0.93
$0.121 \to 0.133$	1.3	1.5	0.903	0.031	0.903	0.951
$0.125 \to 0.121$	1.3	1.46	0.871	0.012	0.871	0.899
$0.125 \to 0.125$	1.3	1.47	0.876	0.015	0.876	0.909
$0.125 \to 0.129$	1.3	1.49	0.884	0.02	0.884	0.922
$0.125 \to 0.133$	1.3	1.51	0.897	0.028	0.897	0.943
$0.129 \to 0.121$	1.3	1.48	0.864	0.0083	0.864	0.89
$0.129 \to 0.125$	1.3	1.49	0.869	0.012	0.869	0.898
$0.129 \to 0.129$	1.3	1.5	0.877	0.016	0.877	0.911
$0.129 \to 0.133$	1.3	1.52	0.889	0.024	0.889	0.932
$0.133 \to 0.121$	1.3	1.5	0.854	0.003	0.854	0.875
$0.133 \to 0.125$	1.3	1.51	0.859	0.0062	0.859	0.884
$0.133 \to 0.129$	1.3	1.52	0.866	0.011	0.866	0.896
$0.133 \to 0.133$	1.3	1.54	0.878	0.018	0.878	0.916

Table 3: *Radiative and $\mathcal{O}(1/m_Q)$ correction factors for $\omega = 1.2$ and 1.3. (κ_Q and $\kappa_{Q'}$ are the initial and final heavy quark hopping parameters.)*

3 Details of the simulation

Our calculation is performed using 60 $SU(3)$ gauge field configurations generated on a $24^3 \times 48$ lattice at $\beta = 6.2$, using the hybrid over-relaxed algorithm described in Ref. [9]. Since we are studying the decays of quarks whose masses are large in lattice units, we must control discretisation errors. In order to reduce these errors, we use an $\mathcal{O}(a)$-improved fermion action originally proposed by Sheikholeslami and Wohlert[10], given by

$$S_F^{SW} = S_F^W - i\frac{\kappa}{2}\sum_{x,\mu,\nu}\bar{q}(x)F_{\mu\nu}(x)\sigma_{\mu\nu}q(x), \tag{18}$$

where S_F^W is the Wilson action:

$$\begin{aligned} S_F^W = \sum_x \Bigg(\bar{q}(x)q(x) \quad - \quad \kappa\sum_\mu \Big[& \bar{q}(x)(1-\gamma_\mu)U_\mu(x)q(x+\hat{\mu}) \\ + \quad & \bar{q}(x+\hat{\mu})(1+\gamma_\mu)U_\mu^\dagger(x)q(x) \Big] \Bigg) . \end{aligned} \tag{19}$$

The use of the SW action reduces discretisation errors from $\mathcal{O}(ma)$ to $\mathcal{O}(\alpha_s\, ma)$ [10, 11] provided one also uses "improved" operators, for example, those obtained by "rotating" the field of the heavy quark, Q:

$$Q(x) \longrightarrow (1 - \frac{1}{2}\gamma\cdot\vec{D})\, Q(x) \ . \tag{20}$$

Thus, to obtain an $\mathcal{O}(a)$-improved evaluation of the matrix element in Eq. (5), we use a "rotated" improved current

$$J^\mu \equiv \bar{Q}'(x)\tilde{\Gamma}^\mu\, Q(x) \ , \tag{21}$$

where

$$\tilde{\Gamma}^\mu = (1 + \frac{1}{2}\gamma\cdot\overleftarrow{D})\,(1-\gamma^\mu)\gamma_5\,(1 - \frac{1}{2}\gamma\cdot\vec{D}). \tag{22}$$

The gauge field configurations and the light quark propagators were generated on the 64-node i860 Meiko Computing Surface at the University of Edinburgh. The heavy quark propagators were computed using the Cray T3D, also at Edinburgh.

In order to enhance the signal for the baryon correlation functions, the light and heavy quark propagators have been computed using the Jacobi smearing method [12], at both the sink and the source (SS). Since smearing is not a Lorentz-invariant operation, it alters some of the transformation properties of computed quantities. In a previous publication [3], we have shown that such an effect is evident in two-point baryonic correlators at non-zero momentum. In Appendix A, we include a study of the smearing effects for SS three-point functions.

Statistical errors are obtained from a bootstrap procedure [13]. This involves the creation of 1000 bootstrap samples from the original set of 60 configurations by randomly selecting 60 configurations per sample (with replacement). Statistical errors are then obtained from the central 68% of the corresponding bootstrap distributions as detailed in Ref. [14].

3.1 Correlators and details of the analysis

In order to study semileptonic decays of the type $\Lambda_b \to \Lambda_c\, l\, \bar{\nu}_l$ on the lattice, we consider the following three-point correlators:

$$(C(t_x,t_y))_\mu^{Q\to Q'} = \sum_{\vec{x}}\sum_{\vec{y}} e^{-i\vec{p}'\cdot\vec{x}} e^{-i\vec{q}\cdot\vec{y}} \langle \mathcal{O}^{Q'}(x)(J_\mu(y))^{Q\to Q'}\bar{\mathcal{O}}^{Q}(0)\rangle \tag{23}$$

where the spinorial indices are implicit. The operator

$$\mathcal{O}^Q(x) = \epsilon_{abc}(l_1^{aT}\mathcal{C}\gamma_5 l_2^b)Q^c \tag{24}$$

is the interpolating operator for the Λ baryon, and the current which mediates the decay of a heavy quark Q into a second heavy quark Q' is given in Eq. (21). l_1 and l_2 represent light quark fields. The three-point function $(C(t_x,t_y))_\mu^{Q\to Q'}$ can be written in terms of quark propagators, as

$$(C(t_x,t_y))_\mu^{Q\to Q'} = -\langle \sum_{\vec{y}} (\Sigma^{c'd}(0,y;t_x,\vec{p})_{Q'}\Gamma_\mu S_Q^{dc'}(y,0)) e^{-i\vec{q}\cdot\vec{y}}\rangle, \tag{25}$$

where $S_Q^{dc}(y,0)$ is the propagator of the Q quark from y to the origin in the presence of a background field configuration,

$$\Sigma^{cd}(0,y;t_x,\vec{p})_{Q'} = \epsilon_{abc}\epsilon_{a'b'c'}\sum_{\vec{x}} e^{-i\vec{p}'\cdot\vec{x}} \mathrm{Tr}\Big[S_{l_1}^{aa'\ T}(x,0)\mathcal{C}\gamma_5 S_{l_2}^{bb'}(x,0)\gamma_5\mathcal{C}\Big] S_{Q'}^{cd}(x,y) \tag{26}$$

where T represents the transpose in spinor-space, $\langle..\rangle$ denotes the average over gluon configurations, and a,b,c,d,a',b',c' are colour indices. S_{l_1} and S_{l_2} are the propagators of the two light quarks. The extended propagator (26) can be evaluated using the standard source method reviewed in Ref. [15].

In the limit of large t_x and $t_x - t_y$ (in the forward part of the lattice), where the ground state contributions to the correlation function should dominate, we can rewrite the correlator as follows [2]

$$(C(t_x,t_y))_\mu^{Q\to Q'} = \frac{ZZ'}{4EE'} e^{-E'(t_x-t_y)} e^{-Et_y}\left((\not{p}' + M')\mathcal{F}_\mu^{Q',Q}(\not{p}+M)\right), \tag{27}$$

[2]This and the following expressions are only correct in the case in which local operators are used. The actual case of smeared-smeared correlators, which is discussed in Appendix A, is more complicated but conceptually similar.

where

$$\begin{array}{rclcrcl} E &=& \sqrt{M^2+|\vec{p}|^2} & & E' &=& \sqrt{M'^{\,2}+|\vec{p}-\vec{q}|^2} \\ M &=& M_{\Lambda(Q)} & & M' &=& M_{\Lambda(Q')} \\ p_\mu &=& (E,\vec{p}) & & p'_\mu &=& (E',\vec{p}-\vec{q}) \\ Z &=& Z(\Lambda(Q),|\vec{p}|) & & Z' &=& Z(\Lambda(Q'),|\vec{p}-\vec{q}|). \end{array} \tag{28}$$

The weak matrix element can be written in terms of the six lattice form factors,

$$\langle \Lambda^{(r)}_{Q'}(\vec{p}\,')|(J_\mu(0,\vec{0}))^{Q\to Q'}|\Lambda^{(s)}_{Q}(\vec{p})\rangle = \bar{u}^{(r)}_{Q'}(\vec{p}\,')\mathcal{F}^{Q',Q}_\mu(p',p)u^{(s)}_Q(\vec{p}) \tag{29}$$

$$\begin{array}{rcl} \text{with} \qquad \mathcal{F}^{Q',Q}_\mu(p',p) &=& \left(F^L_1(\omega)\gamma_\mu + F^L_2(\omega)v_\mu + F^L_3(\omega)v'_\mu\right) \\ &-& \left(G^L_1(\omega)\gamma_\mu + G^L_2(\omega)v_\mu + G^L_3(\omega)v'_\mu\right)\gamma_5 \end{array} \tag{30}$$

where $u^{(s),(r)}_{Q(Q')}$ are the spinors of the heavy baryons and s and r are helicity indices. The lattice form factors F^L_i and G^L_i are related to the physical form factors F_i and G_i through the renormalisation constants of the lattice vector and axial current, respectively. This will be discussed in some detail below.

4 Details of the numerical analysis

In this section we describe our procedure for the extraction of the form factors from the lattice correlation functions.

4.1 Analysis of two-point correlation functions at non-zero momentum

The wave-function factors Z, Z' and the energies which appear in Eq. (27) can be obtained from the analysis of the appropriate two-point correlation functions:

$$C^Q_2(\vec{p},t) = \sum_{\vec{x}} e^{-i\vec{p}\cdot\vec{x}}\langle \mathcal{O}^Q(\vec{x},t)\overline{\mathcal{O}}^Q(\vec{0},0)\rangle. \tag{31}$$

This correlator was evaluated for four values of the heavy-quark hopping parameter corresponding to masses around that of the charm quark, and for three combinations of the light-quark masses, as shown in Table (4). We have computed the correlator for momenta up to $|\vec{p}| = 2p_{\min}$, where $p_{\min} = 2\pi/La = \pi/12a$ is the minimum non-zero momentum allowed on our lattice. For the analysis, equivalent momenta have been averaged to reduce the statistical fluctuations.

For the actual case of smeared-smeared operators (see Appendix A), for large time separations and imposing antiperiodic boundary conditions in time, the correlator

κ_{l1}/κ_{l2}	κ_Q			
0.14144/0.14144	0.121	0.125	0.129	0.133
0.14144/0.14226	-	-	0.129	-
0.14226/0.14226	-	-	0.129	-

Table 4: *Quark hopping parameter combinations used in the calculation of baryon two-point functions. (κ_{l1} and κ_{l2} are the two light-quark hopping parameters and κ_Q, that of the heavy quark.)*

C_2^Q becomes

$$C_2^Q(t,\vec{p}) = \\ Z_s^2(|\vec{p}|)\left\{e^{-Et}\left[\frac{E+M-\alpha^2(E-M)}{4E}\mathbb{1} + \frac{E+M+\alpha^2(E-M)}{4E}\gamma_0 - \frac{2\alpha}{4E}\vec{p}\cdot\vec{\gamma}\right]\right. \\ \left. -e^{-E(T-t)}\left[\frac{E+M-\alpha^2(E-M)}{4E}\mathbb{1} - \frac{E+M+\alpha^2(E-M)}{4E}\gamma_0 - \frac{2\alpha}{4E}\vec{p}\cdot\vec{\gamma}\right]\right\}, \tag{32}$$

where p^μ is defined in (28), $\tilde{p}^\mu = (E, -\vec{p})$ is the 4-momentum of the antibaryon propagating in the backward part of the lattice, and Z_s, α are the amplitudes of the smeared operator (defined in Eqs. (81) and (83)).

At zero momentum, the analysis is particularly simple since the only non-zero components are independent of the unphysical amplitude α. Details of this case are given in Ref. [3]. At finite momentum, we have used both the diagonal and the off-diagonal components of the spinorial matrix to extract the energy from the exponential fall-off. The values of the amplitudes Z_s and α were obtained by fitting separately the contributions proportional to the identity, to γ_0 and to γ_i, and by taking suitable linear combinations of the overall factors, as explained in the appendix of Ref. [3]. The results of these fits, for those mass combinations which are relevant to the present study, and for momenta up to $|\vec{p}| = \sqrt{2}\pi/12a$ are reported in Tables 5 and 6.

The case corresponding to $\kappa_{l1} = \kappa_{l2} = 0.14144$ is further studied in detail to check the precision with which the dispersion relations are satisfied as the momentum of the baryon is increased. It is nowadays customary [16, 17] to replace the continuum dispersion relation (cdr)

$$a^2E^2 = a^2m^2 + p^2a^2 \tag{33}$$

with the so-called lattice dispersion relation (ldr)

$$a^2E^2 = a^2m^2 + \sin^2(pa), \tag{34}$$

which is suggested by the form of the free fermionic propagator on a discrete lattice. For the heavy-quark masses in Table 5 the two dispersion relations yield

κ_{l1}/κ_{l2}	κ_Q	$\vec{p}=(0,0,0)$	$\vec{p}=(\frac{2\pi}{La},0,0)$	$\vec{p}=(\frac{2\pi}{La},\frac{2\pi}{La},0)$
0.14144/0.14144	0.121	$1.138\ ^{+7}_{-7}$	$1.167\ ^{+9}_{-9}$	$1.192\ ^{+13}_{-12}$
	0.125	$1.040\ ^{+6}_{-6}$	$1.072\ ^{+9}_{-9}$	$1.099\ ^{+13}_{-12}$
	0.129	$0.938\ ^{+6}_{-6}$	$0.973\ ^{+8}_{-7}$	$1.002\ ^{+13}_{-13}$
	0.133	$0.829\ ^{+6}_{-6}$	$0.868\ ^{+8}_{-7}$	$0.901\ ^{+14}_{-13}$
0.14144/0.14226	0.129	$0.910\ ^{+8}_{-7}$	$0.943\ ^{+9}_{-9}$	$0.972\ ^{+12}_{-14}$
0.14226/0.14226	0.129	$0.876\ ^{+9}_{-8}$	$0.914\ ^{+10}_{-10}$	$0.948\ ^{+17}_{-17}$
chiral/chiral	0.129	$0.807\ ^{+15}_{-10}$		
chiral/strange	0.129	$0.853\ ^{+14}_{-\ 6}$		

Table 5: *Energies of the Λ-baryon in lattice units for all the momenta and quark hopping parameters relevant to the present study.*

	$\vec{p}=(0,0,0)$	$\vec{p}=(p_{\min},0,0)$		$\vec{p}=(p_{\min},p_{\min},0)$	
κ_Q	$Z_s^2\times 10^4$	$Z_s^2\times 10^4$	α	$Z_s^2\times 10^4$	α
$(\kappa_{l1},\kappa_{l2})=(0.14144,0.14144)$					
0.121	$4.44\ ^{+48}_{-38}$	$2.85\ ^{+40}_{-32}$	$0.66\ ^{+7}_{-7}$	$1.96\ ^{+42}_{-32}$	$0.56\ ^{+9}_{-8}$
0.125	$4.41\ ^{+48}_{-37}$	$2.86\ ^{+40}_{-32}$	$0.70\ ^{+7}_{-7}$	$1.95\ ^{+40}_{-32}$	$0.60\ ^{+10}_{-\ 8}$
0.129	$4.35\ ^{+45}_{-36}$	$2.84\ ^{+35}_{-30}$	$0.77\ ^{+7}_{-7}$	$1.94\ ^{+40}_{-32}$	$0.66\ ^{+11}_{-\ 9}$
0.133	$4.17\ ^{+41}_{-35}$	$2.75\ ^{+34}_{-28}$	$0.83\ ^{+7}_{-8}$	$1.87\ ^{+40}_{-31}$	$0.73\ ^{+13}_{-11}$
$(\kappa_{l1},\kappa_{l2})=(0.14144,0.14226)$					
0.129	$4.02\ ^{+42}_{-36}$	$2.56\ ^{+36}_{-29}$	$0.76\ ^{+8}_{-8}$	$1.68\ ^{+39}_{-30}$	$0.68\ ^{+13}_{-11}$
$(\kappa_{l1},\kappa_{l2})=(0.14226,0.14226)$					
0.129	$3.77\ ^{+87}_{-75}$	$2.42\ ^{+38}_{-32}$	$0.71\ ^{+9}_{-8}$	$1.60\ ^{+45}_{-33}$	$0.65\ ^{+15}_{-12}$

Table 6: *Amplitudes Z_s and α obtained from the analysis of the finite momentum two-point functions.*

essentially indistinguishable results for the energy at $|\vec{p}| = p_{\rm min}$. In addition, the theoretical predictions coincide with the measured values, confirming that the systematic effects at this low value of the momentum are negligible. For momentum $|\vec{p}| = \sqrt{2}p_{\rm min}$, we note that the predicted value is about 1% larger than the measured one, although always compatible within one sigma. Given this result, it seems that the correction obtained with the lattice dispersion relation goes in the right direction. However, much more precise data are needed to draw a firm conclusion on this issue.

Finally, for the conversion of our values for masses and energies into physical units we need an estimate of the inverse lattice spacing in GeV. Following Ref. [3], we use the value given in Eq. (17). The error in Eq. (17) is large enough to encompass all our estimates for a^{-1} from quantities such as m_ρ, f_π, m_N, the string tension $\sqrt{K}$ and the hadronic scale R_0 discussed in [18].

4.2 Three-point functions and lattice form factors

In this subsection we explain our procedure for extracting the form factors from the computed three-point (and two-point) correlation functions. We have computed the three-point functions for the mass combinations tabulated in Table 7. In order to study the dependence of the form factors on the masses of the heavy quarks, we have computed the correlation functions for all combinations of κ_Q and $\kappa_{Q'}$ taken from 0.121, 0.125, 0.129, 0.133, but with the light-quark masses fixed by $\kappa_{l1} = \kappa_{l2} = 0.14144$ (which is close to that of the strange quark). On the other hand, the dependence on the light-quark masses was studied by keeping fixed the mass of the initial and final heavy quarks $\kappa_Q = \kappa_{Q'} = 0.129$ which is very close to that of the charm quark, and considering the three light hopping-parameter combinations $\kappa_{l1} = \kappa_{l2} = 0.14144$, $\kappa_{l1} = 0.14226, \kappa_{l2} = 0.14144$, and $\kappa_{l1} = \kappa_{l2} = 0.14226$. In light of the encouraging results obtained below, we envisage the possibility of repeating the calculation on a larger sample of heavy- and light-quark masses.

We measure the six form factors for the different quark masses from the three-point functions (23), whose expression, for large values of t_x and $t_x - t_y$ in the forward part of the lattice and for local interpolating operators was given in Eq. (27). The more complicated case of SS correlators, which is explained in detail in Appendix A, can be written schematically as follows:

$$\begin{aligned}(C(t))_\mu^{Q\to Q'} &= \frac{ZZ'}{16EE'}e^{-E'(T/2-t)}e^{-Et}\times\Big[\mathcal{V}_\mu(\alpha,\beta,M,M',\vec{p},\vec{p}')\ F_1^L(\omega)\\ &+ \mathcal{W}(\alpha,\beta,M,M',\vec{p},\vec{p}')\Big(v_\mu F_2^L(\omega)+v'_\mu F_3^L(\omega)\Big)\\ &- \mathcal{A}_\mu(\alpha,\beta,M,M',\vec{p},\vec{p}')\ G_1^L(\omega)\\ &+ \mathcal{B}(\alpha,\beta,M,M',\vec{p},\vec{p}')\Big(v_\mu G_2^L(\omega)+v'_\mu G_3^L(\omega)\Big)\Big] \qquad (35)\end{aligned}$$

κ_{l1}/κ_{l2}	$\kappa_Q \rightarrow \kappa_{Q'}$			
	degenerate transitions			
0.14144/ 0.14144	$0.121 \rightarrow 0.121$	$0.125 \rightarrow 0.125$	$0.129 \rightarrow 0.129$	$0.133 \rightarrow 0.133$
0.14144/ 0.14226	-	$0.129 \rightarrow 0.129$	-	-
0.14226/ 0.14226	-	$0.129 \rightarrow 0.129$	-	-
	non-degenerate transitions			
0.14144/ 0.14144		$0.121 \rightarrow 0.125$	$0.121 \rightarrow 0.129$	$0.121 \rightarrow 0.133$
	$0.125 \rightarrow 0.121$	-	$0.125 \rightarrow 0.129$	$0.135 \rightarrow 0.133$
	$0.129 \rightarrow 0.121$	$0.129 \rightarrow 0.125$	-	$0.133 \rightarrow 0.133$
	$0.133 \rightarrow 0.121$	$0.133 \rightarrow 0.125$	$0.133 \rightarrow 0.129$	-

Table 7: *Quark hopping parameter combinations used in the calculation of baryon three-point functions. (κ_{l1} and κ_{l2} are the two light-quark hopping parameters while κ_Q and $\kappa_{Q'}$ are those of the initial and final heavy quarks.)*

where we have set $t_x = T/2$ (which is the value we chose in our computations), and have renamed the remaining time variable $t_y \rightarrow t$. The matrices $\mathcal{V}, \mathcal{W}, \mathcal{A}, \mathcal{B}$ are different linear combinations of the Dirac matrices, with coefficients which depend on the arguments shown. The overall normalisation factor, as well as the four matrices $\mathcal{V}, \mathcal{W}, \mathcal{A}, \mathcal{B}$ can be fully reconstructed from the two-point functions at the corresponding values of the masses and momenta, as illustrated in Section 4.1.

We will now consider separately the two cases in which we keep either the axial or vector currents from the $V - A$ current which mediates the semileptonic weak decays of heavy baryons. The following discussion is based on equations (85) and (86) in Appendix A.

4.2.1 Analysis of the axial form factors

The freedom to choose the Lorentz index μ and the spinor components appropriately allows us to extract the required form factors efficiently [3]. It is convenient to think of the four-by-four spinorial matrix as subdivided into four two-by-two matrices, as explained in Appendix B. We find that

[3] Alternatively we could use suitable projection operators in spinor space.

1. *current indices* $\mu = i$ *with* $i = 1, 2, 3$: the large components[4] of $\mathcal{A}_i$ are located in the top (bottom) diagonal submatrix in the forward (backward) part of the lattice. The large components of $\mathcal{B}$ are located in the top-right (bottom-left) corner submatrix. Thus the contributions of the form factor G_1^L can be separated from that of $G_{2,3}^L$.

2. *current index* $\mu = 0$: the large components of both $\mathcal{A}_0$ and $\mathcal{B}$ are located in the top-right (bottom-left) corner matrices in the forward (backward) part of the lattice. So the three form factors contribute to the same spinorial components, making the extraction of the form factors very uncertain. Therefore, the equations obtained from the current with index $\mu = 0$ will not be considered in the analysis below.

We conclude that from an analysis of the correlators with index $\mu = 1, 2, 3$, it is possible to obtain a clean straightforward determination of the form factors. We consider the asymptotic form of Eq. (35), fitting for either G_1^L or $G_{2,3}^L$ separately, depending on the particular spinorial component under study.

Once the time-dependent factor in (35) has been divided out, we observe long and stable plateaux, centered around $t = 12$. As an example we exhibit in Figures 1A and 1B, the plateaux for the form factors G_1^L and G_2^L, for one set of masses and choice of momenta. We have fitted G_1^L for 3, 5 and 7 timeslices. The central values of the fits are insensitive to the choice of fitting interval, and in order to avoid possible contaminations due to exited states, we have decided to restrict the fitting range to three time slices centered around $t = 12$. The $\chi^2_{\rm dof}$ for these fits were always very reasonable, ranging from $\chi^2_{\rm dof} \sim 0.5$ to $\chi^2_{\rm dof} \sim 2$.

As was discussed in Section 2, the form factors are related to the physical renormalized Isgur-Wise function through a multiplicative renormalisation which takes into account the short-distance QCD corrections. Furthermore an additional renormalisation constant (Z_A) must be introduced in order to relate the lattice improved axial current (22) to the continuum one. Perturbative and non-perturbative calculations of Z_A are available in the literature [19, 20], but it can also be estimated non-perturbatively in this computation. As can be seen from Eqs. (14), G_1 reduces to the Isgur-Wise function, at zero recoil, and it is free from $\mathcal{O}(1/m_Q)$ corrections because of Luke's theorem. If we make the reasonable assumption that $\mathcal{O}(1/m_Q^2)$ corrections are small, a measure of $G_1^L(1)/N_1^5(1)$ will

[4]Here and in the following, we refer to the numerical coefficients of the form factors in Eq. (35) as *large* if they are proportional to the energy or mass of the baryon, and as small if they are proportional to the spatial momentum p.

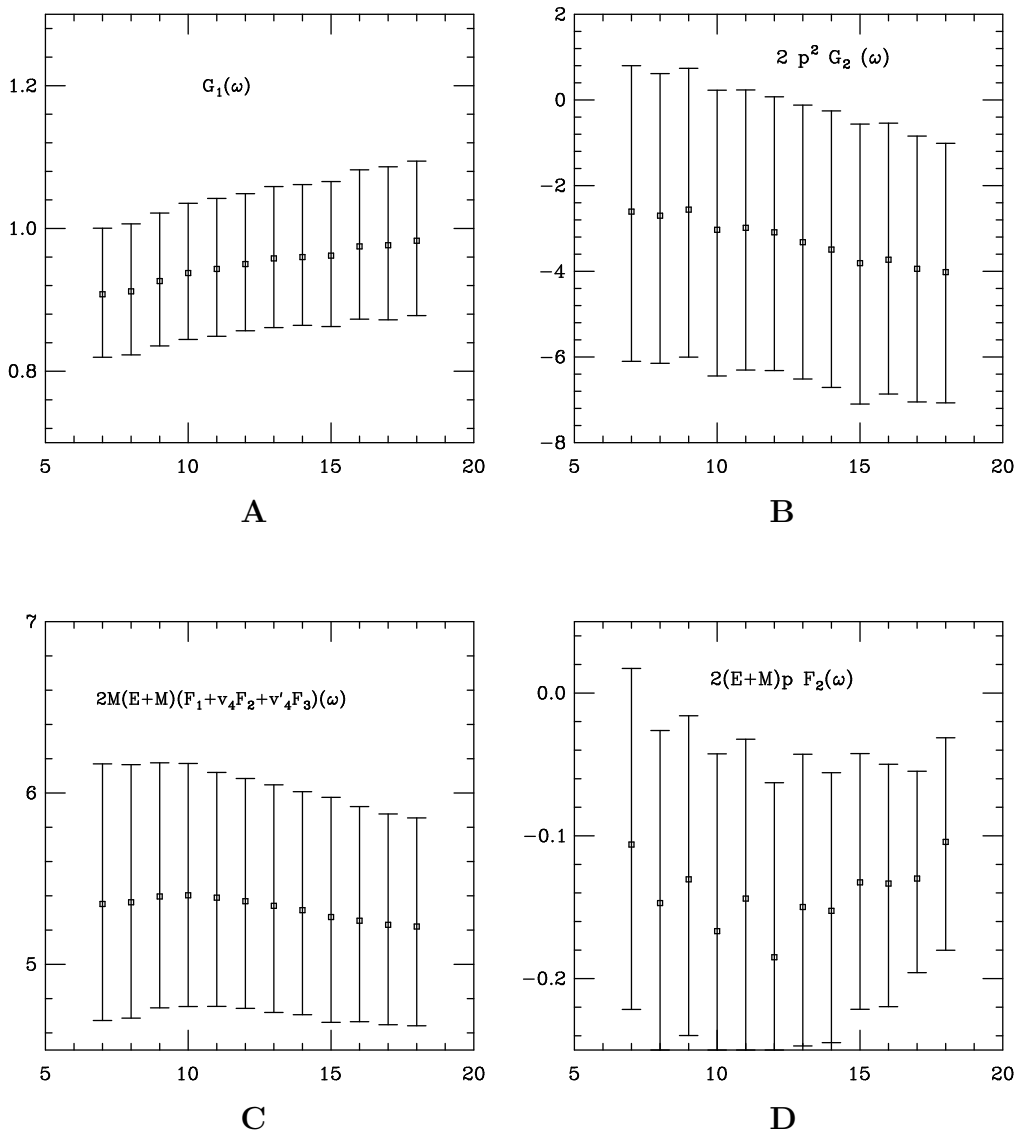

Figure 1: *Examples of the plateaux used in the fit to (from left to right, top to bottom)* $G_1(\omega)$, $G_2(\omega)$, $\sum_i F_i(\omega)$ *and* $F_2(\omega)$. $\kappa_{l1} = \kappa_{l2} = 0.14144$, $\kappa_Q = \kappa_{Q'} = 0.121$, *the initial particle is at rest and the final particle has momentum* $(p', 0, 0)$, *where* $p' = 2\pi/La$.

give us a non-perturbative estimate of Z_A^{-1}. For degenerate transitions,

$$\begin{aligned}
\frac{N_1^5(1)}{G_1^L(1)} &= 0.98\ {}^{+8}_{-8} \quad \text{at} \qquad \kappa_{l1} = \kappa_{l2} = 0.14144, \text{and } \kappa_h = 0.133 \\
\frac{N_1^5(1)}{G_1^L(1)} &= 0.97\ {}^{+8}_{-8} \quad \text{at} \qquad \kappa_{l1} = \kappa_{l2} = 0.14144, \text{and } \kappa_h = 0.129 \\
\frac{N_1^5(1)}{G_1^L(1)} &= 0.98\ {}^{+9}_{-8} \quad \text{at} \qquad \kappa_{l1} = \kappa_{l2} = 0.14144, \text{and } \kappa_h = 0.125 \\
\frac{N_1^5(1)}{G_1^L(1)} &= 0.98\ {}^{+10}_{-9} \quad \text{at} \qquad \kappa_{l1} = \kappa_{l2} = 0.14144, \text{and } \kappa_h = 0.121\,,
\end{aligned} \tag{36}$$

to be compared with the non-perturbative estimate of Z_A, obtained for light quarks [20]

$$Z_A^{\text{non-pert}} = 1.04\ {}^{+1}_{-1}. \tag{37}$$

The coefficients N_1^5 used in Eqs. (36) were computed from expressions (12). Within the statistical precision of our calculation, we have no evidence of discretisation errors nor of $\mathcal{O}(1/m_Q^2)$ corrections (assuming that these two effects do not partially cancel, which is very unlikely give the range of masses we consider). Indeed, we observe that the four values in (36) are exceptionally stable with the quark mass.

In Tables 8, 9 and 10, we present our results, for the quantity

$$\hat{\xi}_{QQ'}(\omega) = \frac{G_1^L(\omega)}{G_1^L(1)} \times \frac{N_1^5(1)}{N_1^5(\omega)} \tag{38}$$

for all the quark masses and for initial and final momenta up to $|\vec{p}|, |\vec{p}\,'| = \sqrt{2}$. It follows from the above discussion that this quantity is independent of the lattice renormalisation constant Z_A.

$\kappa_{l1} = 0.14144, \qquad \kappa_{l2} = 0.14144$

$\vec{p}, \vec{p}\,'$	$0.121 \to 0.121$		$0.121 \to 0.125$		$0.121 \to 0.129$		$0.121 \to 0.133$	
$[p_{\min}]$	ω	$\hat{\xi}_{QQ'}$	ω	$\hat{\xi}_{QQ'}$	ω	$\hat{\xi}_{QQ'}$	ω	$\hat{\xi}_{QQ'}$
(0,0,0), (1,0,0)	1.026	$0.97\,^{+3}_{-3}$	1.030	$0.96\,^{+3}_{-3}$	1.037	$0.94\,^{+4}_{-3}$	1.048	$0.91\,^{+4}_{-4}$
(0,0,0), (1,1,0)	1.050	$0.95\,^{+6}_{-8}$	1.060	$0.93\,^{+7}_{-8}$	1.073	$0.91\,^{+8}_{-7}$	1.09	$0.90\,^{+7}_{-8}$
(1,0,0), (0,1,0)	1.052	$0.94\,^{+11}_{-12}$	1.057	$0.92\,^{+10}_{-10}$	1.064	$0.91\,^{+12}_{-9}$	1.07	$0.89\,^{+10}_{-8}$
(1,0,0), (1,0,0)	1.000	$1.02\,^{+10}_{-11}$	1.000	$0.95\,^{+11}_{-12}$	1.001	$0.94\,^{+12}_{-12}$	1.003	$0.93\,^{+12}_{-12}$
(1,0,0), (-1,0,0)	1.10	$0.81\,^{+9}_{-8}$	1.11	$0.76\,^{+9}_{-8}$	1.13	$0.74\,^{+9}_{-7}$	1.15	$0.70\,^{+8}_{-7}$
(1,0,0), (0,0,0)	-	-	1.026	$0.95\,^{+4}_{-5}$	1.026	$0.95\,^{+5}_{-4}$	1.026	$0.95\,^{+5}_{-4}$
(1,0,0), (0,1,1)	1.077	$0.95\,^{+2}_{-2}$	1.09	$0.92\,^{+17}_{-16}$	1.10	$0.88\,^{+18}_{-15}$	1.12	$0.80\,^{+17}_{-15}$

Table 8: *Estimates of the function $\hat{\xi}_{QQ'}$ as obtained from the axial form factor G_1. All the transitions, corresponding to initial heavy $\kappa = 0.121$ and 0.125 and initial and final momenta up to $|\vec{p}|, |\vec{p}\,'| = \sqrt{2} p_{\min}$ are shown. Statistical errors in ω are in the last digit or beyond.*

$\kappa_{l1} = 0.14144, \qquad \kappa_{l2} = 0.14144$

$\vec{p}, \vec{p}\,'$	$0.125 \to 0.125$		$0.125 \to 0.121$		$0.125 \to 0.129$		$0.125 \to 0.133$	
$[p_{\min}]$	ω	$\hat{\xi}_{QQ'}$	ω	$\hat{\xi}_{QQ'}$	ω	$\hat{\xi}_{QQ'}$	ω	$\hat{\xi}_{QQ'}$
(0,0,0), (1,0,0)	1.030	$0.95\,^{+3}_{-3}$	1.026	$0.99\,^{+2}_{-3}$	1.037	$0.94\,^{+4}_{-3}$	1.048	$0.91\,^{+5}_{-4}$
(0,0,0), (1,1,0)	1.060	$0.95\,^{+6}_{-8}$	1.050	$0.96\,^{+6}_{-8}$	1.073	$0.93\,^{+8}_{-7}$	1.09	$0.89\,^{+8}_{-7}$
(1,0,0), (0,1,0)	1.062	$0.91\,^{+10}_{-10}$	1.057	$0.92\,^{+10}_{-10}$	1.069	$0.89\,^{+11}_{-8}$	1.08	$0.87\,^{+10}_{-8}$
(1,0,0), (1,0,0)	1.000	$1.02\,^{+10}_{-11}$	1.000	$0.97\,^{+11}_{-12}$	1.000	$0.95\,^{+13}_{-11}$	1.002	$0.94\,^{+13}_{-12}$
(1,0,0), (-1,0,0)	1.12	$0.76\,^{+8}_{-8}$	1.11	$0.75\,^{+10}_{-8}$	1.14	$0.71\,^{+9}_{-6}$	1.16	$0.67\,^{+8}_{-6}$
(1,0,0), (0,0,0)	-	-	1.030	$0.94\,^{+5}_{-5}$	1.030	$0.94\,^{+6}_{-4}$	1.030	$0.94\,^{+5}_{-4}$
(1,0,0), (0,1,1)	1.09	$0.90\,^{+17}_{-16}$	1.08	$0.91\,^{+17}_{-16}$	1.11	$0.85\,^{+18}_{-15}$	1.13	$0.78\,^{+17}_{-14}$

Table 8: *(continued)*

$\kappa_{l1} = 0.14144, \qquad \kappa_{l2} = 0.14144$

$\vec{p}, \vec{p}\,'$	$0.133 \to 0.133$		$0.133 \to 0.121$		$0.133 \to 0.125$		$0.133 \to 0.129$	
$[p_{\min}]$	ω	$\hat{\xi}_{QQ'}$	ω	$\hat{\xi}_{QQ'}$	ω	$\hat{\xi}_{QQ'}$	ω	$\hat{\xi}_{QQ'}$
(0,0,0), (1,0,0)	1.048	$0.91\,^{+3}_{-3}$	1.026	$1.02\,^{+2}_{-3}$	1.030	$1.00\,^{+3}_{-3}$	1.037	$0.96\,^{+3}_{-3}$
(0,0,0), (1,1,0)	1.09	$0.82\,^{+6}_{-8}$	1.050	$0.96\,^{+7}_{-7}$	1.08	$0.97\,^{+7}_{-7}$	1.073	$0.93\,^{+6}_{-7}$
(1,0,0), (0,1,0)	1.10	$0.82\,^{+9}_{-8}$	1.074	$0.88\,^{+10}_{-9}$	1.07	$0.87\,^{+10}_{-8}$	1.09	$0.85\,^{+9}_{-8}$
(1,0,0), (1,0,0)	1.000	$1.02\,^{+12}_{-13}$	1.003	$0.98\,^{+12}_{-11}$	1.002	$0.98\,^{+13}_{-12}$	1.001	$0.97\,^{+12}_{-13}$
(1,0,0), (-1,0,0)	1.20	$0.57\,^{+6}_{-6}$	1.15	$0.69\,^{+10}_{-7}$	1.16	$0.67\,^{+9}_{-7}$	1.173	$0.63\,^{+7}_{-6}$
(1,0,0), (0,0,0)	-	-	1.048	$0.90\,^{+6}_{-6}$	1.048	$0.91\,^{+6}_{-5}$	1.048	$0.92\,^{+5}_{-5}$
(1,0,0), (0,1,1)	1.15	$0.71\,^{+14}_{-13}$	1.100	$0.83\,^{+16}_{-14}$	1.111	$0.80\,^{+16}_{-13}$	1.13	$0.76\,^{+15}_{-14}$

Table 9: *Estimates of the function $\hat{\xi}_{QQ'}$ as obtained from the axial form factor G_1. All the transitions, corresponding to initial heavy $\kappa = 0.133$ and 0.129 and initial and final momenta up to $|\vec{p}|, |\vec{p}\,'| = \sqrt{2} p_{\min}$ are shown. Statistical errors in ω are in the last digit or beyond.*

$\kappa_{l1} = 0.14144, \qquad \kappa_{l2} = 0.14144$

$\vec{p}, \vec{p}\,'$	$0.129 \to 0.129$		$0.129 \to 0.121$		$0.129 \to 0.125$		$0.129 \to 0.133$	
$[p_{\rm min}]$	ω	$\hat{\xi}_{QQ'}$	ω	$\hat{\xi}_{QQ'}$	ω	$\hat{\xi}_{QQ'}$	ω	$\hat{\xi}_{QQ'}$
(0,0,0), (1,0,0)	1.037	$0.94\,^{+3}_{-3}$	1.026	$1.01\,^{+3}_{-3}$	1.030	$0.98\,^{+3}_{-3}$	1.048	$0.91\,^{+4}_{-4}$
(0,0,0), (1,1,0)	1.073	$0.93\,^{+6}_{-8}$	1.050	$0.97\,^{+8}_{-7}$	1.060	$0.96\,^{+7}_{-7}$	1.09	$0.88\,^{+6}_{-8}$
(1,0,0), (0,1,0)	1.076	$0.88\,^{+9}_{-9}$	1.064	$0.91\,^{+11}_{-9}$	1.069	$0.89\,^{+10}_{-8}$	1.09	$0.84\,^{+8}_{-8}$
(1,0,0), (1,0,0)	1.000	$1.02\,^{+11}_{-11}$	1.001	$0.98\,^{+12}_{-11}$	1.000	$0.97\,^{+13}_{-12}$	1.001	$0.96\,^{+13}_{-13}$
(1,0,0), (-1,0,0)	1.15	$0.68\,^{+7}_{-6}$	1.13	$0.72\,^{+10}_{-7}$	1.14	$0.71\,^{+9}_{-7}$	1.17	$0.63\,^{+6}_{-6}$
(1,0,0), (0,0,0)	-	-	1.037	$0.92\,^{+6}_{-5}$	1.037	$0.92\,^{+6}_{-4}$	1.037	$0.92\,^{+4}_{-4}$
(1,0,0), (0,1,1)	1.11	$0.81\,^{+16}_{-14}$	1.09	$0.89\,^{+17}_{-14}$	1.10	$0.86\,^{+17}_{-14}$	1.13	$0.74\,^{+14}_{-14}$

Table 9: *(continued)*

We observe that:

- Our determinations of $\hat{\xi}_{QQ'}(\omega)$ have statistical errors ranging from 3 to 15%. As a general rule, we note that for the same heavy-quark masses, errors increase with the momentum of the final baryon. Furthermore, errors are amplified as the light quarks approach the chiral limit.
- The estimates of $\hat{\xi}_{QQ'}(\omega)$ obtained from transitions with final momentum $|\vec{p}\,'| = \sqrt{2}p_{\rm min}$ are in agreement with those of similar ω obtained from channels with lower momentum. However, since these points are more affected by discretisation errors, we do not include them in our determination of the Isgur-Wise function.

The estimates reported in Tables 8 and 9 are also plotted in Figure 2, for all the degenerate and non-degenerate transitions, at $\kappa_{l1} = \kappa_{l2} = 0.14144$. We have included all the points obtained from baryons either at rest or with momenta $|\vec{p}|, |\vec{p}\,'| = p_{\rm min}$. The interpretation of the dependence of $\hat{\xi}_{QQ'}(\omega)$ on the velocity transfer is postponed to Section 5.1.

We conclude this section with a comment on the determination of the suppressed form factors G_2^L and G_3^L. As can be observed from Figure 1B, the signal is very noisy and compatible with zero. Because of this feature, which is common to

$0.129 \to 0.129$

$\vec{p},\vec{p}\,'$ $[p_{\min}]$	$\kappa_{l1}=0.14144,\ \kappa_{l2}=0.14226$ ω	$\hat{\xi}_{QQ'}$	$\kappa_{l1}=0.14226,\ \kappa_{l2}=0.14226$ ω	$\hat{\xi}_{QQ'}$
(0,0,0), (1,0,0)	1.040	$0.92\,^{+3}_{-4}$	1.043	$0.92\,^{+5}_{-6}$
(0,0,0), (1,1,0)	1.078	$0.95\,^{+6}_{-9}$	1.084	$0.98\,^{+7}_{-10}$
(1,0,0), (0,1,0)	1.081	$0.85\,^{+12}_{-11}$	1.088	$0.80\,^{+18}_{-15}$
(1,0,0), (1,0,0)	1.000	$1.02\,^{+11}_{-11}$	1.000	$0.85\,^{+24}_{-25}$
(1,0,0), (-1,0,0)	1.16	$0.68\,^{+9}_{-9}$	1.18	$0.72\,^{+13}_{-12}$
(1,0,0), (0,1,1)	1.121	$0.77\,^{+20}_{-19}$	1.131	$0.59\,^{+27}_{-25}$

Table 10: *Estimates of the function $\hat{\xi}_{QQ'}$ as obtained from the axial form factor G_1. All the degenerate transitions $\kappa_Q = \kappa_{Q'} = 0.129$ and light masses corresponding to $\kappa_{l1}, \kappa_{l2} = 0.14144, 0.14226$ and $0.14226, 0.14226$ with initial and final momenta up to $|\vec{p}|, |\vec{p}\,'| = \sqrt{2}p_{\min}$ are shown. Statistical errors in ω are in the last digit or beyond.*

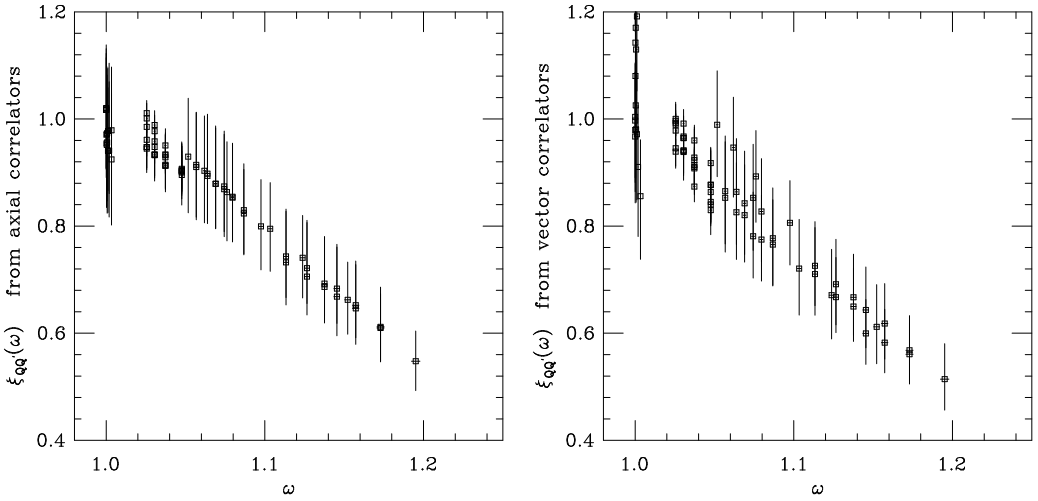

Figure 2: *$\hat{\xi}_{QQ'}(\omega)$, as obtained from axial (left) and vector (right) current matrix elements.*

most of the momentum channels, we are unable to determine these form factors, within the available statistics.

4.2.2 Analysis of the vector form factors

The analysis of the vector form factors proceeds along the same lines as those followed for the axial form factors, with some significant differences. It is interesting to measure not only the three form factors F_i^L, with $i = 1, 2, 3$, separately, but also their sum because of the normalisation condition (14). Indeed, as we will see below, it proves to be easier to determine the sum precisely than the individual form factors.

We now study the different spinor components of the two matrices $\mathcal{V}_\mu, \mathcal{W}$ for different values of the index μ. As was the case for the axial current, the discussion is based on equations (85) and (86) in Appendix A. We find that

1. *for indices $\mu = i$ with $i = 1, 2, 3$:* the large components of $\mathcal{V}_i$ are located in the top-right (bottom-left) submatrix in the forward (backward) part of the lattice, whereas the non-vanishing components of $\mathcal{W}$ are located along the diagonal. Thus, the form factors F_1^L and $F_{2,3}^L$ give separate contributions to different spinorial components. However, as shown in Appendix B, spinorial components located in the off-diagonal submatrices are always proportional to the amplitudes α and β and thus are noisier than those located in the diagonal submatrices. From this feature we can already anticipate that the determination of F_1^L is going to be less precise than that of G_1^L.

2. *for current indices $\mu = 0$:* the large components of both $\mathcal{V}_\mu$ and $\mathcal{W}$ are located in the top (bottom)-diagonal submatrix in the forward (backward) part of the lattice. In this case one obtains the linear combination of the three form factors $F_1^L + v_0\, F_2^L + v_0'\, F_3^L$ which is approximately equal to $F_1 + F_2 + F_3$ at the low momenta which we are using. These channels have a very clean and precise signal, which is the reason for the accurate determination of the sum of the form factors.

In view of the above discussion, it has proved to be advantageous to consider equations both with $\mu = i$ and with $\mu = 0$, minimizing the full covariance matrix with respect to the three form factors, and reconstructing their sum. Examples of plateaux obtained from channels with $\mu = 0$ and with $\mu = i$ are shown in Figures 1C and 1D, respectively. As expected, the relative statistical error is smaller in the first case, and we find that the stability and symmetry of the plateau is also better. In extracting the values of the form factors we have again restricted the fitting range to three time slices centered around $t = 12$, and we find very reasonable values of $\chi^2_{\rm dof}$. Confirming the indications of the preliminary

discussion above, we measure F_1^L, F_2^L and F_3^L individually with relatively large statistical errors, ranging from 6 to 20%, whereas the errors on their sum are never more than 10%.

In order to extract the form factors from the correlation functions measured on the lattice it is necessary to determine the renormalisation constant Z_V which relates the lattice and physical vector currents. This constant has previously been determined non-perturbatively, by studying the matrix elements of the charge operator between meson states, and the results are reviewed in Appendix C. Noting that for degenerate transitions between baryon states at rest, $Z_V\, V_0^L$ is the charge operator, we find here that

$$1 = Z_V(\sum_i F_i^L(1)) \ . \tag{39}$$

The numerical values of Z_V obtained in this way are:

$$\begin{aligned}
Z_V &= 0.84\ ^{+7}_{-6} \quad \text{at} \quad \kappa_{l1} = \kappa_{l2} = 0.14144 \text{ and } \kappa_h = 0.133 \\
Z_V &= 0.85\ ^{+8}_{-7} \quad \text{at} \quad \kappa_{l1} = \kappa_{l2} = 0.14144 \text{ and } \kappa_h = 0.129 \\
Z_V &= 0.87\ ^{+9}_{-7} \quad \text{at} \quad \kappa_{l1} = \kappa_{l2} = 0.14144 \text{ and } \kappa_h = 0.125 \\
Z_V &= 0.88\ ^{+9}_{-8} \quad \text{at} \quad \kappa_{l1} = \kappa_{l2} = 0.14144 \text{ and } \kappa_h = 0.121
\end{aligned} \tag{40}$$

which are in agreement with the other non-perturbative estimates presented in Appendix C, obtained with a different method. Below we will use $1/\sum_i F_i(1)$ to normalise the lattice vector current.

In Tables 11, 12 and 13, we present our results for the quantity

$$\hat{\xi}_{QQ'}(\omega) = \frac{F_1^L(\omega) + F_2^L(\omega) + F_3^L(\omega)}{\sum_i F_i^L(1)} \frac{N_{\rm sum}(1)}{N_{\rm sum}(\omega)} \tag{41}$$

for all the combinations of quark masses and for initial and final momenta up to $|\vec{p}|, |\vec{p}\,'| = p_{\rm min}$. The results reported in Tables 11 and 12 are also plotted in Figure 2, for all the degenerate and non-degenerate transitions, at $\kappa_{l1} = \kappa_{l2} = 0.14144$. The study of the dependence of $\hat{\xi}_{QQ'}(\omega)$ on the velocity transfer is again postponed to Section 5.1.

We end this subsection with a discussion of the determination of the form factors F_1, F_2 and F_3 separately. The form factors F_2 and F_3 start at $\mathcal{O}(\alpha_s)$ in perturbation theory and at next-to-leading order in the $1/m_Q$ expansion and they are thus expected to be small relative to F_1 and sensitive to the values of the heavy-quark masses (which in the present study vary by almost a factor two: $m_q \in [1.48, 2.38]$). In Figure 3, we plot our estimates of

$$F_{2,3}(\omega) = F_{2,3}^L(\omega)\, \frac{N_{\rm sum}(1)}{\sum_i F_i^L(1)}. \tag{42}$$

$\kappa_{l1} = 0.14144, \qquad \kappa_{l2} = 0.14144$

$\vec{p}, \vec{p}\,'$	$0.121 \to 0.121$		$0.121 \to 0.125$		$0.121 \to 0.129$		$0.121 \to 0.133$	
$[p_{\min}]$	ω	$\hat{\xi}_{QQ'}$	ω	$\hat{\xi}_{QQ'}$	ω	$\hat{\xi}_{QQ'}$	ω	$\hat{\xi}_{QQ'}$
(0,0,0), (1,0,0)	1.026	$1.00\ ^{+3}_{-3}$	1.030	$0.94\ ^{+4}_{-5}$	1.037	$0.91\ ^{+3}_{-4}$	1.048	$0.84\ ^{+4}_{-4}$
(1,0,0), (0,1,0)	1.052	$0.99\ ^{+10}_{-9}$	1.057	$0.87\ ^{+10}_{-10}$	1.064	$0.83\ ^{+9}_{-9}$	1.074	$0.79\ ^{+9}_{-8}$
(1,0,0), (1,0,0)	1.000	$1.00\ ^{+10}_{-11}$	1.000	$1.08\ ^{+12}_{-13}$	1.001	$0.97\ ^{+11}_{-13}$	1.003	$0.86\ ^{+11}_{-12}$
(1,0,0), (-1,0,0)	1.103	$0.73\ ^{+9}_{-9}$	1.113	$0.74\ ^{+8}_{-7}$	1.127	$0.67\ ^{+7}_{-7}$	1.145	$0.61\ ^{+6}_{-6}$
(1,0,0), (0,0,0)	-	-	1.026	$0.99\ ^{+4}_{-5}$	1.026	$0.98\ ^{+4}_{-4}$	1.026	$0.95\ ^{+3}_{-4}$
$\vec{p}, \vec{p}\,'$	$0.125 \to 0.125$		$0.125 \to 0.121$		$0.125 \to 0.129$		$0.125 \to 0.133$	
$[p_{\min}]$	ω	$\hat{\xi}_{QQ'}$	ω	$\hat{\xi}_{QQ'}$	ω	$\hat{\xi}_{QQ'}$	ω	$\hat{\xi}_{QQ'}$
(0,0,0), (1,0,0)	1.030	$0.99\ ^{+2}_{-3}$	1.026	$0.94\ ^{+2}_{-3}$	1.037	$0.92\ ^{+3}_{-4}$	1.048	$0.85\ ^{+4}_{-4}$
(1,0,0), (0,1,0)	1.062	$0.95\ ^{+9}_{-9}$	1.057	$0.86\ ^{+10}_{-10}$	1.069	$0.83\ ^{+9}_{-9}$	1.080	$0.78\ ^{+8}_{-8}$
(1,0,0), (1,0,0)	1.000	$1.00\ ^{+11}_{-12}$	1.000	$1.14\ ^{+13}_{-14}$	1.000	$1.03\ ^{+11}_{-14}$	1.002	$0.91\ ^{+11}_{-13}$
(1,0,0), (-1,0,0)	1.124	$0.68\ ^{+8}_{-8}$	1.113	$0.72\ ^{+8}_{-7}$	1.138	$0.66\ ^{+7}_{-6}$	1.157	$0.59\ ^{+5}_{-6}$
(1,0,0), (0,0,0)	-	-	1.030	$0.94\ ^{+5}_{-6}$	1.030	$0.97\ ^{+4}_{-4}$	1.030	$0.94\ ^{+4}_{-4}$

Table 11: *Estimates of the function $\hat{\xi}_{QQ'}$ as obtained from the vector form factor combination $\sum_i F_i$. All the transitions, corresponding to initial heavy $\kappa = 0.121$ and 0.125 and initial and final momenta up to $|\vec{p}|, |\vec{p}\,'| = \sqrt{2} p_{\min}$ are shown. Statistical errors in ω are in the last digit or beyond.*

$\kappa_{l1} = 0.14144, \qquad \kappa_{l2} = 0.14144$

$\vec{p}, \vec{p}\,'$	$0.129 \to 0.129$		$0.129 \to 0.121$		$0.129 \to 0.125$		$0.129 \to 0.133$	
$[p_{\min}]$	ω	$\hat{\xi}_{QQ'}$	ω	$\hat{\xi}_{QQ'}$	ω	$\hat{\xi}_{QQ'}$	ω	$\hat{\xi}_{QQ'}$
(0,0,0), (1,0,0)	1.037	$0.96\ ^{+3}_{-3}$	1.026	$1.00\ ^{+2}_{-2}$	1.030	$0.97\ ^{+2}_{-3}$	1.048	$0.83\ ^{+5}_{-5}$
(1,0,0), (0,1,0)	1.076	$0.90\ ^{+8}_{-8}$	1.064	$0.87\ ^{+10}_{-10}$	1.069	$0.85\ ^{+10}_{-9}$	1.087	$0.77\ ^{+8}_{-8}$
(1,0,0), (1,0,0)	1.000	$0.98\ ^{+11}_{-12}$	1.001	$1.19\ ^{+13}_{-14}$	1.000	$1.17\ ^{+13}_{-14}$	1.001	$0.98\ ^{+13}_{-14}$
(1,0,0), (-1,0,0)	1.152	$0.62\ ^{+8}_{-7}$	1.127	$0.70\ ^{+8}_{-7}$	1.138	$0.68\ ^{+8}_{-7}$	1.173	$0.57\ ^{+6}_{-5}$
(1,0,0), (0,0,0)	-	-	1.037	$0.93\ ^{+6}_{-6}$	1.037	$0.93\ ^{+5}_{-6}$	1.037	$0.91\ ^{+4}_{-4}$
$\vec{p}, \vec{p}\,'$	$0.133 \to 0.133$		$0.133 \to 0.121$		$0.133 \to 0.125$		$0.133 \to 0.129$	
$[p_{\min}]$	ω	$\hat{\xi}_{QQ'}$	ω	$\hat{\xi}_{QQ'}$	ω	$\hat{\xi}_{QQ'}$	ω	$\hat{\xi}_{QQ'}$
(0,0,0), (1,0,0)	1.048	$0.92\ ^{+3}_{-3}$	1.026	$1.00\ ^{+2}_{-2}$	1.030	$0.96\ ^{+2}_{-2}$	1.037	$0.88\ ^{+2}_{-3}$
(1,0,0), (0,1,0)	1.098	$0.82\ ^{+8}_{-8}$	1.074	$0.86\ ^{+10}_{-9}$	1.080	$0.84\ ^{+10}_{-9}$	1.087	$0.79\ ^{+9}_{-9}$
(1,0,0), (1,0,0)	1.000	$0.97\ ^{+12}_{-12}$	1.003	$1.21\ ^{+13}_{-15}$	1.002	$1.20\ ^{+13}_{-15}$	1.001	$1.13\ ^{+13}_{-14}$
(1,0,0), (-1,0,0)	1.195	$0.53\ ^{+6}_{-6}$	1.145	$0.66\ ^{+8}_{-7}$	1.157	$0.63\ ^{+7}_{-6}$	1.173	$0.58\ ^{+6}_{-6}$
(1,0,0), (0,0,0)	-	-	1.048	$0.88\ ^{+7}_{-7}$	1.048	$0.88\ ^{+6}_{-6}$	1.048	$0.87\ ^{+5}_{-5}$

Table 12: *Estimates of the function $\hat{\xi}_{QQ'}$ as obtained from the vector form factor combination $\sum_i F_i$. All the transitions, corresponding to initial heavy $\kappa = 0.133$ and 0.129 and initial and final momenta up to $|\vec{p}|, |\vec{p}\,'| = \sqrt{2} p_{\min}$ are shown. Statistical errors in ω are in the last digit or beyond.*

$0.129 \to 0.129$

$\vec{p},\vec{p}\,'$ $[p_{\rm min}]$	$\kappa_{l1}=0.14144,\ \kappa_{l2}=0.14226$ ω	$\hat{\xi}_{QQ'}$	$\kappa_{l1}=0.14226,\ \kappa_{l2}=0.14226$ ω	$\hat{\xi}_{QQ'}$
(0,0,0), (1,0,0)	1.040	$0.95\ ^{+3}_{-4}$	1.043	$0.93\ ^{+5}_{-5}$
(1,0,0), (0,1,0)	1.081	$0.87\ ^{+10}_{-11}$	1.088	$0.77\ ^{+14}_{-13}$
(1,0,0), (1,0,0)	1.000	$0.86\ ^{+16}_{-15}$	1.000	$0.63\ ^{+27}_{-26}$
(1,0,0), (-1,0,0)	1.16	$0.62\ ^{+9}_{-8}$	1.18	$0.64\ ^{+13}_{-10}$

Table 13: *Estimates of the function $\hat{\xi}_{QQ'}$ as obtained from the form factor $\sum_i F_i$. All the degenerate transitions $\kappa_Q = \kappa_{Q'} = 0.129$ and light masses corresponding to $\kappa_{l1}, \kappa_{l2} = 0.14144, 0.14226$ and $0.14226, 0.14226$ with initial and final momenta up to $|\vec{p}|, |\vec{p}\,'| = \sqrt{2}p_{\rm min}$ are shown. Statistical errors in ω are in the last digit or beyond.*

We observe that these form factors are small and negative as one would expect from Eq. (12). Our measurements of

$$F_1(\omega) = F_1^L(\omega)\,\frac{N_{\rm sum}(1)}{\sum_i F_i^L(1)} \tag{43}$$

for degenerate transitions are also presented in Figure 3. In order to decrease the number of parameters in the fit, we restricted the analysis to degenerate transitions, for which one can use the symmetry relation $F_2(\omega) = F_3(\omega)$.

As anticipated above, the errors in the individual form factors are larger than that in their sum. To make this clear, we plot in Figure 4 the form factors F_1, F_2 and the sum, $F_1 + 2F_2$, for the degenerate channel with heavy quark hopping parameter $\kappa_Q = 0.121$. It can be seen that the fluctuations in F_1 and F_2 partially compensate each other in the determination of the function $\hat{\xi}_{QQ'}$

A more detailed discussion of the behavior of both F_1 and $F_{2,3}$ and of their relation with the Isgur-Wise function, will be presented in Section 5.1.

5 The Isgur-Wise function

In this section we study the dependence of the function $\hat{\xi}_{QQ'}(\omega)$ on the masses of the initial and final heavy quarks so as to extract the corresponding Isgur-Wise

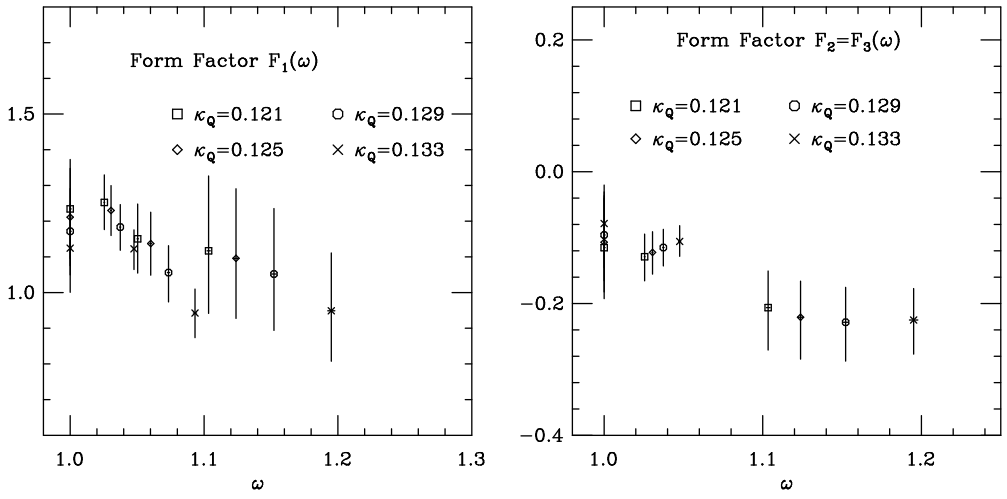

Figure 3: *Form factors F_1 and $F_2 = F_3$, as obtained from degenerate quark transitions. Different symbols correspond to different heavy-quark hopping parameters. The light-quark hopping parameters are always $\kappa_{l1} = \kappa_{l2} = 0.14144$.*

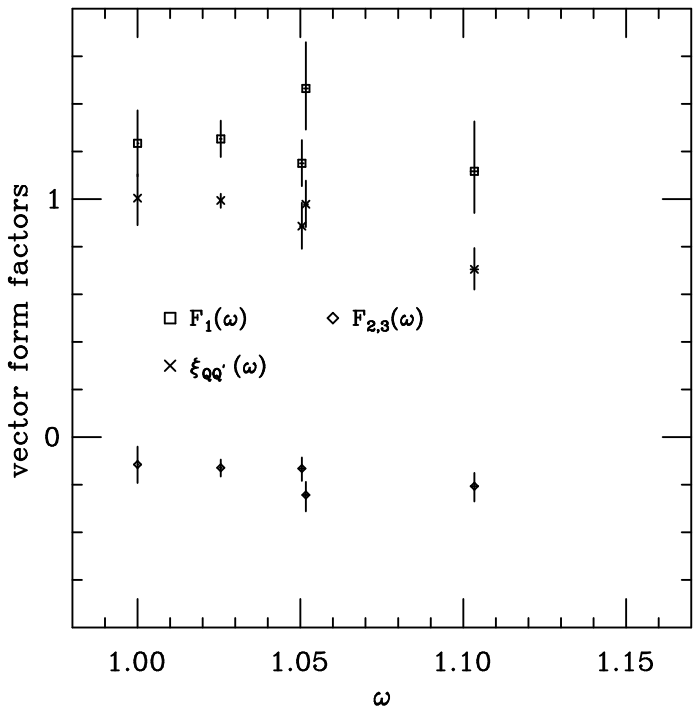

Figure 4: *Example of the relative size of the normalized vector form factors. $\kappa_{l1} = \kappa_{l2} = 0.14144$ and $\kappa_Q = \kappa_{Q'} = 0.121$.*

function. We also study its dependence on the velocity transfer ω, and the mass of the light quarks. We further attempt to estimate the size of $1/m_Q$ corrections.

5.1 $\hat{\xi}_{QQ'}(\omega)$ as a function of ω and of heavy-quark mass

As discussed in Section 2, both the axial form factor G_1 and the sum of the vector form factors $\sum_i F_i$, are protected from $1/m_Q$ corrections at zero recoil (see Eq. (14)). Away from zero recoil, these quantities are no longer protected by Luke's theorem and they suffer $1/m_Q$ corrections. We recall their expansion in powers of the inverse heavy-quark mass, given in Eqs. (11) and (9)

$$\begin{aligned}\frac{G_1(\omega)}{N_1^5(\omega)} &= \frac{\sum_i F_i(\omega)}{N_{\rm sum}(\omega)} = \hat{\xi}_{QQ'}(\omega) \\ &= \xi^{\rm ren}(\omega) + \left(\frac{\bar{\Lambda}}{2m_Q} + \frac{\bar{\Lambda}}{2m_{Q'}}\right)\left[\frac{(\omega-1)}{(\omega+1)}\xi^{\rm ren}(\omega) + 2\chi^{\rm ren}(\omega)\right] \\ &\quad + \mathcal{O}\left(1/m^2_{Q^{(\prime)}}\right). \end{aligned} \tag{44}$$

In this section we study the dependence of the form factors on ω in order to extract some phenomenologically interesting quantities. In particular, the slope of $\hat{\xi}_{QQ'}(\omega)$ at zero recoil can be related to the slope of the physical form factors (see also Section 6) through the correction coefficients given in Eqs. (11) and (12). The form factors, in turn, are needed in the calculation of the decay rates and asymmetry parameters.

In order to obtain reliable estimates of phenomenological quantities, we must learn how to extrapolate our data, obtained for initial and final heavy quarks with masses around that of the charm quark, to the physical $b \to c$ decays. HQET provides us with the guide for this extrapolation, and it is important to understand the rôle of the $1/m_Q$ corrections, present in the function (44), and to check that higher-order corrections are small.

With the aim of reducing the statistical error we exploit the relation (44), and fit the vector and axial data together. This is correct up to terms of $\mathcal{O}(1/m_Q^2)$ and two-loop perturbative corrections, which we neglect throughout this study. Near $\omega = 1$ we expand $\hat{\xi}_{QQ'}(\omega)$ as a linear function of ω

$$\hat{\xi}_{QQ'}(\omega) = 1 - \rho^2(\omega - 1) + \mathcal{O}\left((\omega-1)^2\right) \ , \tag{45}$$

and we study whether there is any dependence of the slope, ρ^2, on the masses of the heavy quarks. Our results are obtained for the set of initial- and final-state heavy-quark masses given in Table 7, but with fixed light-quark masses around that of the strange ($\kappa_{l1} = \kappa_{l2} = 0.14144$). It can be seen from Figure 5 that there is no statistical evidence of a dependence of $\hat{\xi}_{QQ'}(\omega)$ on the heavy-quark mass. In

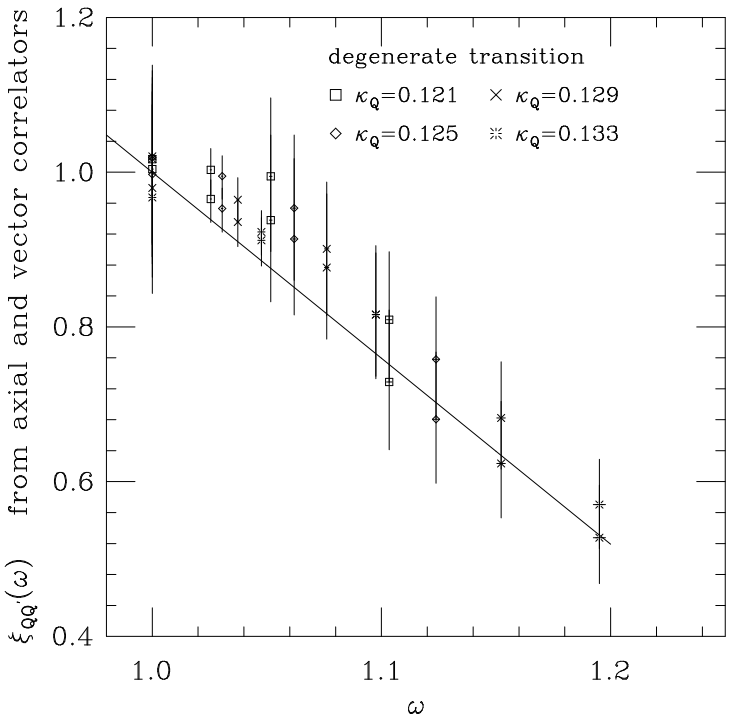

Figure 5: $\hat{\xi}_{QQ'}(\omega)$ *from degenerate transitions, using vector and axial current data. Different graphical symbols denote different heavy quark masses, which appear to follow the same curve.*

order to quantify this statement, we have fitted separately to the function (45), each of the four data sets corresponding to degenerate transitions obtaining

$$\begin{aligned}
\rho^2 &= 2.4\ {}^{+3}_{-3} \qquad \text{at} \qquad \kappa_Q = \kappa_{Q'} = 0.121 \\
\rho^2 &= 2.4\ {}^{+3}_{-4} \qquad \text{at} \qquad \kappa_Q = \kappa_{Q'} = 0.125 \\
\rho^2 &= 2.4\ {}^{+4}_{-4} \qquad \text{at} \qquad \kappa_Q = \kappa_{Q'} = 0.129 \\
\rho^2 &= 2.4\ {}^{+4}_{-4} \qquad \text{at} \qquad \kappa_Q = \kappa_{Q'} = 0.133,
\end{aligned} \tag{46}$$

confirming that no dependence on the heavy-quark mass can be detected.

Our conclusion from this analysis is that our data for $\hat{\xi}_{QQ'}(\omega)$ do not show any evidence of sizable $1/m_Q$ corrections, within our precision. So even though $\hat{\xi}_{QQ'}(\omega)$ is not, in principle, a universal function, it appears to be a good approximation to the Isgur-Wise function. Thus, from now on, we will consider $\hat{\xi}_{QQ'}(\omega)$ to be our estimate of the Isgur-Wise function, $\xi^{\rm ren}(\omega)$.

For the slope of the Isgur-Wise function corresponding to light-quark masses around that of the strange we take the result in Eq. (46), which will be used later to study the $1/m_Q$ corrections to the individual vector form factors. This choice

is motivated by the fact that the analysis of the $1/m_Q$ corrections is based on the data obtained from degenerate transitions.

5.2 $\xi^{\rm ren}(\omega)$ as a function of the light-quark masses

The Isgur-Wise function depends on the quantum numbers of the light degrees of freedom, i.e. on the so-called "brown muck". Previous studies on the lattice [21] demonstrated that such a dependence is not negligible in the case of mesons, where the brown muck contains only one light quark. Thus we might expect to measure an even stronger dependence of the baryonic Isgur-Wise function on the masses of the light quarks, and we investigate whether this is the case in the present subsection.

We study the dependence of $\xi^{\rm ren}(\omega)$ on the light quarks by keeping the masses of the heavy quarks fixed at $\kappa_Q = \kappa_{Q'} = 0.129$ and letting the light quarks take the three values listed in Table 7. By simultaneously fitting $G_1(\omega)$ and $\sum_i F_i(\omega)$ to Eq. (45), we find:

$$\begin{aligned}
\rho^2 &= 2.4\ {}^{+4}_{-4} \qquad \text{at} \qquad \kappa_{l1} = 0.14144, \quad \kappa_{l2} = 0.14144 \\
\rho^2 &= 2.0\ {}^{+5}_{-5} \qquad \text{at} \qquad \kappa_{l1} = 0.14144, \quad \kappa_{l2} = 0.14226 \\
\rho^2 &= 1.7\ {}^{+6}_{-8} \qquad \text{at} \qquad \kappa_{l1} = 0.14226, \quad \kappa_{l2} = 0.14226
\end{aligned} \tag{47}$$

The comparison between these fits and the data is shown in Figures 6, for all three combinations of light-quark masses and also for the results extrapolated to the chiral limit.

In order to obtain the slope ρ^2 in the chiral limit, we extrapolate the three estimates of both ω and $\xi^{\rm ren}(\omega)$ obtained with $\kappa_Q = \kappa_{Q'} = 0.129$ and with the combinations of light-quark masses in Eq. (47). We assume that ω and $\xi^{\rm ren}(\omega)$ depend linearly on the sum of the two light-quark masses, that is

$$\omega(\kappa_Q, \kappa_{l1}, \kappa_{l2}) = \omega(\kappa_Q) + C\left(\frac{1}{2\kappa_{l1}} + \frac{1}{2\kappa_{l2}} - \frac{1}{\kappa_{\rm crit}}\right) \tag{48}$$

and similarly for $\xi^{\rm ren}$. This assumption is supported by our results for the spectrum presented in Ref. [3]. The results of the extrapolation to the chiral limit, which are relevant for the semileptonic decay $\Lambda_b \to \Lambda_c l\bar{\nu}$, are presented in Table 14 and in Figure 6. Our best estimate of the slope of the renormalized Isgur-Wise function for the Λ_b baryon is

$$\rho^2 = 1.2 + 0.8 - 1.1\ . \tag{49}$$

Using the functional form (48), we also obtain the values of ω and $\xi^{\rm ren}(\omega)$ for the semileptonic decay $\Xi_b \to \Xi_c l\bar{\nu}$, interpolating to one strange and extrapolating to

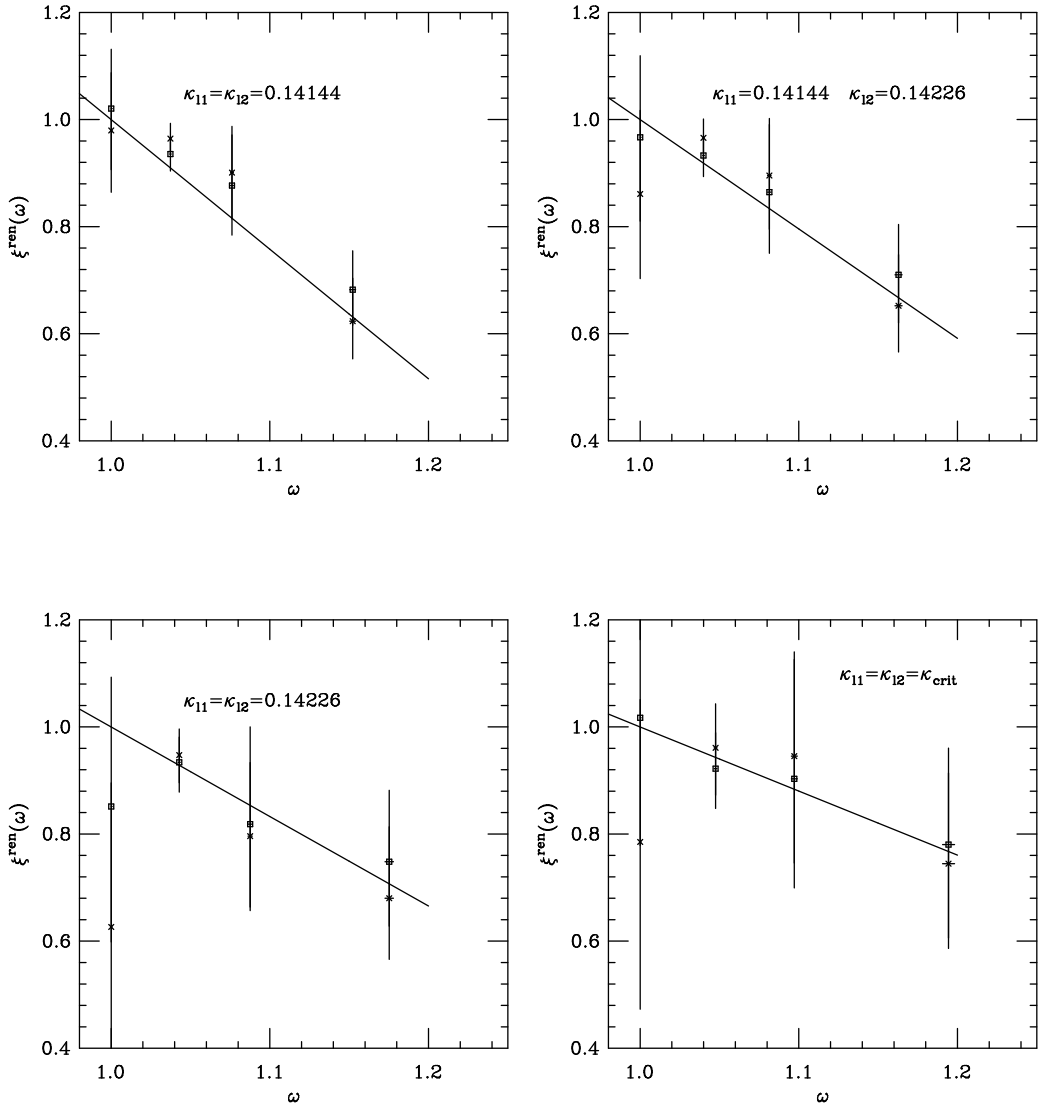

Figure 6: *Plot of the Isgur-Wise function at fixed heavy-quark masses ($\kappa_Q = \kappa_{Q'} = 0.129$) and various light quark masses, down to the chiral limit. Both vector (crosses) and axial (boxes) determinations were used for the fits.*

κ_{l1}/κ_{l2}	ω	$\xi^{\rm ren}$ (A)	$\xi^{\rm ren}$ (V)
0.14144/0.4144	1.0	$1.02\ ^{+11}_{-11}$	$0.98\ ^{+11}_{-12}$
	$1.0373\ ^{+4}_{-5}$	$0.94\ ^{+3}_{-3}$	$0.96\ ^{+3}_{-3}$
	$1.0761\ ^{+9}_{-9}$	$0.88\ ^{+9}_{-9}$	$0.90\ ^{+8}_{-8}$
	$1.152\ ^{+2}_{-2}$	$0.68\ ^{+7}_{-6}$	$0.62\ ^{+8}_{-7}$
0.14144/0.14226	1.0	$0.97\ ^{+15}_{-16}$	$0.86\ ^{+16}_{-17}$
	$1.0399\ ^{+5}_{-5}$	$0.93\ ^{+3}_{-4}$	$0.97\ ^{+3}_{-4}$
	$1.081\ ^{+1}_{-1}$	$0.86\ ^{+12}_{-11}$	$0.90\ ^{+10}_{-10}$
	$1.163\ ^{+2}_{-2}$	$0.71\ ^{+9}_{-9}$	$0.65\ ^{+9}_{-8}$
0.14226/0.14226	1.0	$0.85\ ^{+24}_{-25}$	$0.63\ ^{+27}_{-27}$
	$1.0429\ ^{+6}_{-6}$	$0.93\ ^{+5}_{-6}$	$0.95\ ^{+5}_{-5}$
	$1.088\ ^{+1}_{-1}$	$0.82\ ^{+18}_{-15}$	$0.80\ ^{+13}_{-14}$
	$1.175\ ^{+3}_{-3}$	$0.75\ ^{+13}_{-12}$	$0.68\ ^{+13}_{-11}$
Chiral/Chiral	1.0	$1.02\ ^{+23}_{-24}$	$0.79\ ^{+26}_{-32}$
	$1.0475\ ^{+9}_{-9}$	$0.92\ ^{+7}_{-7}$	$0.96\ ^{+8}_{-9}$
	$1.097\ ^{+2}_{-2}$	$0.90\ ^{+22}_{-20}$	$0.95\ ^{+19}_{-19}$
	$1.194\ ^{+4}_{-4}$	$0.78\ ^{+17}_{-17}$	$0.74\ ^{+16}_{-15}$
Chiral/Strange	1.0	$1.03\ ^{+18}_{-19}$	$0.87\ ^{+22}_{-22}$
	$1.0439\ ^{+8}_{-8}$	$0.93\ ^{+5}_{-6}$	$0.96\ ^{+6}_{-6}$
	$1.090\ ^{+2}_{-2}$	$0.90\ ^{+17}_{-16}$	$0.92\ ^{+16}_{-15}$
	$1.179\ ^{+3}_{-4}$	$0.75\ ^{+13}_{-13}$	$0.70\ ^{+12}_{-12}$

Table 14: *Estimates of* $\xi^{\rm ren}(\omega)$ *from both axial (A) and vector (V) form factors, at* $\kappa_Q = \kappa_{Q'} = 0.129$ *and for three combinations of the light-quark masses, as well as at the physical limits. The results at* $\omega = 1$ *correspond to those from the momentum channel* $(1,0,0) \to (1,0,0)$.

one chiral quark. The numerical results are also presented in Table 14. Our best estimate for the slope for the Ξ_b baryon is

$$\rho^2 = 1.5\ {}^{+7}_{-9}\ . \tag{50}$$

In this exploratory study we have only used a very limited set of light-quark masses, and hence our conclusions on the dependence of the Isgur-Wise function on these masses are rather weak, and the extrapolation to the chiral limit is not very precise. This should be remedied in future simulations.

5.3 $\mathcal{O}(1/m_Q)$ corrections.

In this section we attempt to extract a value of $\bar{\Lambda}$ for the Λ baryon, from the study of the $1/m_Q$ corrections in the vector form factors $F_1(\omega)$ and $F_{2,3}(\omega)$. We start by recalling the relevant expressions given in Section 2

$$\begin{aligned} F_1(\omega) &= N_1(\omega)\hat{\xi}_{QQ'}(\omega) + \mathcal{O}\left(1/m^2_{Q^{(\prime)}}\right) \\ F_2(\omega) &= F_3(\omega) = N_2(\omega)\hat{\xi}_{QQ'}(\omega) + \mathcal{O}\left(1/m^2_{Q^{(\prime)}}\right) \end{aligned} \tag{51}$$

the last equality being valid in the limit of equal heavy-quark masses, to which the present discussion is restricted. Also in this limit, we have

$$\begin{aligned} N_1(\omega) &= \hat{C}_1(\bar{\omega})\left[1 + \frac{2}{\omega+1}\,\frac{\bar{\Lambda}}{m_Q}\right] \\ N_2(\omega) &= \hat{C}_2(\bar{\omega})\left[1 + \frac{\omega-1}{\omega+1}\,\frac{\bar{\Lambda}}{m_Q}\right] - \hat{C}_1(\bar{\omega})\frac{1}{\omega+1}\,\frac{\bar{\Lambda}}{m_Q}. \end{aligned} \tag{52}$$

Combining Eqs. (51) and (52) and using the functions $\hat{\xi}_{QQ'}$ which were determined from the fits to the dominant form factors G_1 and $\sum F_i$ (see Section 5.1), one can view the form factors F_1 and F_2 as functions of $\bar{\Lambda}$ alone. In fact, Eqs. (51) and (52), together with the coefficient functions $\hat{C}_i(\hat{\omega})$, evaluated at one loop order in perturbation theory, can be considered as our definition(s) of the binding energy. As mentioned in Section 2, these form factors are sufficiently sensitive to $\bar{\Lambda}$ for us to attempt an estimate $\bar{\Lambda}$ from the lattice data.

To the order we are working in, the power corrections can be expressed as powers of the inverse quark mass or of the inverse mass of any hadron containing the heavy quark, provided that the same prescription is used in the evaluation of the coefficient functions $\hat{C}_i^{(5)}$. We have decided to use the inverse quark mass, defined as

$$m_Q = M_{\Lambda_Q} - \bar{\Lambda}\ . \tag{53}$$

The analysis is performed using our data for degenerate initial and final heavy quarks ($\kappa_Q = \kappa_{Q'} = 0.121, 0.125, 0.129$ and 0.133) for fixed light-quark masses,

$\kappa_Q \to \kappa_{Q'}$	ω	$\hat{\xi}_{QQ'}$	ω	$\hat{\xi}_{QQ'}$
$0.121 \to 0.121$	1.0	$0.99\ ^{+10}_{-\ 9}$	1.026	$1.02\ ^{+\ 4}_{-\ 3}$
$0.125 \to 0.125$	1.0	$0.95\ ^{+10}_{-\ 9}$	1.030	$0.98\ ^{+3}_{-2}$
$0.129 \to 0.129$	1.0	$0.89\ ^{+10}_{-\ 8}$	1.037	$0.91\ ^{+3}_{-2}$
$0.133 \to 0.133$	1.0	$0.81\ ^{+10}_{-\ 8}$	1.048	$0.83\ ^{+3}_{-3}$
$0.121 \to 0.121$	1.050	$0.95\ ^{+6}_{-6}$	1.103	$0.94\ ^{+18}_{-14}$
$0.125 \to 0.125$	1.060	$0.91\ ^{+6}_{-5}$	1.124	$0.90\ ^{+17}_{-13}$
$0.129 \to 0.129$	1.073	$0.83\ ^{+5}_{-5}$	1.152	$0.85\ ^{+16}_{-12}$
$0.133 \to 0.133$	1.093	$0.71\ ^{+4}_{-4}$	1.195	$0.74\ ^{+14}_{-11}$

Table 15: *$\hat{\xi}_{QQ'}$ as obtained from the form factors F_1 for degenerate heavy quark transitions using Eqs. (51) and (52) and the value of $\bar{\Lambda}$ given in Eq. (54).*

$\kappa_{l1} = \kappa_{l2} = 0.14144$. The fit to $F_1(\omega)$ is good, and we obtain

$$\bar{\Lambda} = 0.75\ ^{+10}_{-13}\ ^{+5}_{-6}\ \text{GeV} \qquad \text{with} \qquad \chi^2_{dof} = 1.0. \tag{54}$$

The less certain fit to $F_2(\omega)$ confirms this value with unexpected precision, given the statistical errors affecting individual points,

$$\bar{\Lambda} = 0.74\ ^{+10}_{-11}\ ^{+5}_{-5}\ \text{GeV} \qquad \text{with} \qquad \chi^2_{dof} = 1.6. \tag{55}$$

In both Eqs. (54) and (55) the first error is statistical and the second is due to the uncertainty in the value of the lattice spacing, see Eq. (17). Using these values of $\bar{\Lambda}$ we evaluate the coefficients $N_{1,2}(\omega)$ and estimate the function $\hat{\xi}_{QQ'}(\omega)$ from the form factors F_1 and F_2 using Eqs. (51). These estimates are presented in Tables 15 and 16, and are compared with the functions $\hat{\xi}_{QQ'}(\omega)$ obtained using the dominant form factors, G_1 and $\sum F_i$, in Figure 7.

Let us comment on the results for the Λ-baryon binding energy.

- As expected, the form factors $F_1(\omega)$ and $F_2(\omega)$ have a significant dependence on the masses of the heavy quarks, a dependence which can be partially understood in terms of the $1/m_Q$ corrections in Eqs. (51) and (52) with the values of $\bar{\Lambda}$ in Eqs. (54) and (55).

- We have neglected all higher-order $1/m_Q$ corrections. These could alter the results of Eqs. (54) and (55) by as much as 30%.

- The separation of $1/m_Q$ corrections from discretisation errors is difficult. Although we have used an improved action to reduce these errors, and have

$\kappa_Q \to \kappa_{Q'}$	ω	$\hat{\xi}_{QQ'}$	ω	$\hat{\xi}_{QQ'}$
$0.121 \to 0.121$	1.0	$0.96\ ^{+52}_{-70}$	1.026	$1.10\ ^{+11}_{-17}$
$0.125 \to 0.125$	1.0	$0.79\ ^{+43}_{-58}$	1.030	$0.92\ ^{+\ 7}_{-12}$
$0.129 \to 0.129$	1.0	$0.61\ ^{+37}_{-45}$	1.037	$0.75\ ^{+52}_{-85}$
$0.133 \to 0.133$	1.0	$0.42\ ^{+30}_{-35}$	1.048	$0.58\ ^{+5}_{-8}$
$0.121 \to 0.121$	1.050	$1.15\ ^{+32}_{-44}$	1.103	$1.87\ ^{+59}_{-66}$
$0.125 \to 0.125$	1.060	$0.91\ ^{+25}_{-36}$	1.124	$1.79\ ^{+53}_{-60}$
$0.129 \to 0.129$	1.073	$0.68\ ^{+20}_{-28}$	1.152	$1.63\ ^{+45}_{-51}$
$0.133 \to 0.133$	1.094	$0.47\ ^{+14}_{-22}$	1.195	$1.38\ ^{+38}_{-40}$

Table 16: $\hat{\xi}_{QQ'}$ *as obtained from the form factors* $F_2 = F_3$ *for degenerate heavy quark transitions using Eqs. (51) and (52) and the value of* $\bar{\Lambda}$ *given in Eq. (55).*

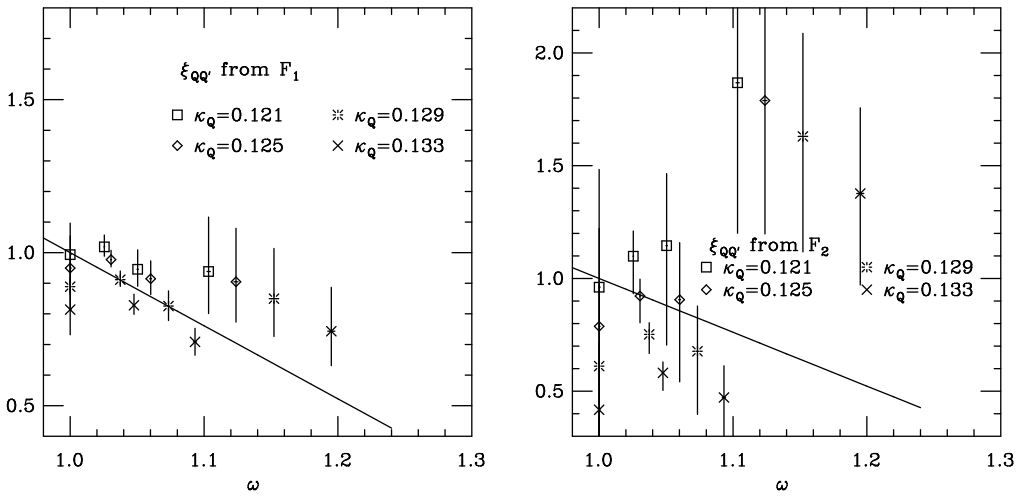

Figure 7: $\hat{\xi}_{QQ'}(\omega)$ *as obtained from the form factors* F_1 *and* $F_2 = F_3$*. The points are compared with the best fit of* $\hat{\xi}_{QQ'}(\omega)$ *obtained previously from the dominant form factors,* G_1 *and* $\sum F_i$*.*

normalized the form factors by Z_V defined by Eq. (39), the stability of the results as the lattice spacing and action are varied should be checked in future simulations. The consistency of the two results (54) and (55) may be evidence that discretisation errors are relatively small.

- Although we have only performed this study with light quarks with masses corresponding to $\kappa_{l1} = \kappa_{l2} = 0.14144$, we can nevertheless calculate $\bar{\Lambda}_\Lambda$ and $\bar{\Lambda}_\Xi$ by using

$$\begin{aligned} \bar{\Lambda} - \bar{\Lambda}_\Lambda &= M_{\rm Baryon} - M_\Lambda + \mathcal{O}(\frac{1}{m_Q}) \\ \text{and} & \\ \bar{\Lambda} - \bar{\Lambda}_\Xi &= M_{\rm Baryon} - M_\Xi + \mathcal{O}(\frac{1}{m_Q}) \ , \end{aligned} \tag{56}$$

  where $\bar{\Lambda}$ and $M_{\rm Baryon}$ are the binding energy and mass of the baryons which we study in our computation. In this way we find:

$$\bar{\Lambda}_\Lambda = 0.37 \ {}^{+11}_{-12} \ \text{GeV} \qquad \text{and} \qquad \bar{\Lambda}_\Xi = 0.50 \ {}^{+11}_{-13} \ \text{GeV} \ , \tag{57}$$

  where statistical and systematic errors have been combined in quadrature. The value of $\bar{\Lambda}_\Lambda$ would correspond to a mesonic binding energy of $\bar{\Lambda}_{\rm mes} \simeq 80 \pm 120\,\text{MeV}$, in agreement, within the large error, with the result quoted in Ref. [8]. The central values of the quark masses obtained using Eq. (57) are different from those used throughout this paper which were obtained from Eq. (16). We have checked that this difference does not noticeably affect the correction coefficients $\hat{C}_i^{(5)}$, and hence our estimates of physical quantities.

- In addition to the systematic uncertainties arising from lattice artefacts, it must be remembered that the computation of power corrections in general is a complicated subject (for a recent review see [22]). In the present case, following standard procedure, we are trying to quantify $1/m_Q$ corrections when we are ignorant of the $\mathcal{O}(\alpha_s^2)$ terms in the perturbation series for the coefficient functions. Although, within our errors, we have found no inconsistencies, we cannot be sure that the values of $\bar{\Lambda}$ would not change significantly if higher-order perturbative terms were included, or that the values would agree with other definitions of $\bar{\Lambda}$.

6 Phenomenological implications

In this section we use the results for the baryonic Isgur-Wise function and for the baryon binding energy $\bar{\Lambda}$ computed above, to obtain the physical form factors

corresponding to the semileptonic decays:

$$\Lambda_b \to \Lambda_c + e\bar{\nu} \qquad \text{and} \qquad \Xi_b \to \Xi_c + e\bar{\nu} \ . \tag{58}$$

We also derive the expressions for the decay rates near zero recoil and use them to make quantitative predictions. We will discuss in detail the decay of the Λ_b; that of the Ξ_b is very similar.

6.1 Physical form factors

The physical form factors can be reconstructed from the computed Isgur-Wise function $\xi^{\rm ren}(\omega)$, using the relations in Eq. (11). In the following we will use the result, discussed in Section 5.1, that the function $\hat{\xi}_{QQ'}(\omega)$ is effectively independent of the mass of the heavy quark. Therefore, the form factors depend on the masses of the heavy quarks only through the correction coefficients $N_i^{(5)}(\omega) = N_i^{(5)}(\omega, m_Q, m_{Q'})$, which are calculated using expressions (12). The short-distance coefficients, $\hat{C}_i^{(5)}(\bar{\omega}, m_b, m_c)$, were computed for $\Lambda_{QCD} = 250$ MeV, $n_f = 4$ and by fixing the quark masses to the values

$$m_b = 4.8 \text{ GeV}, \qquad m_c = 1.45 \text{ GeV}. \tag{59}$$

The factors $\hat{C}_i^{(5)}$ depend on the quark masses very mildly. On the other hand, the correction coefficients $N_i^{(5)}$ are very sensitive to the quark masses, because they contain $1/m_Q$ corrections. In this case, we have expressed m_b and m_c as

$$m_b = M_{\Lambda_b} - \bar{\Lambda} \qquad \text{and} \qquad m_c = M_{\Lambda_c} - \bar{\Lambda} \tag{60}$$

with $M_{\Lambda_b} = 5.64$ GeV and $M_{\Lambda_c} = 2.285$ GeV, respectively. We report our estimates of the correction coefficients $N_i^{(5)}$ for various values of ω, for the Λ and Ξ decays, in Table 17.

It is convenient to expand the physical form factors in $\omega - 1$, near zero recoil:

$$F_i(\omega, m_b, m_c) = \eta_i^V - \tilde{\rho}_i^V(\omega - 1), \qquad G_i(\omega, m_b, m_c) = \eta_i^A - \tilde{\rho}_i^A(\omega - 1); \tag{61}$$

where the normalisations $\eta_i^{V,A}$ and the new slopes are related to the coefficients $N_i^{(5)}$ and to the slope of the Isgur-Wise function by

$$\eta_i^V = N_i(1, m_b, m_c), \quad \eta_i^A = N_i^5(1, m_b, m_c), \tag{62}$$

$$\tilde{\rho}_i^V = \rho^2 \, N_i(1, m_b, m_c) - \left. \frac{dN_i(\omega, m_b, m_c)}{d\omega} \right|_{\omega=1} , \tag{63}$$

and

$$\tilde{\rho}_i^A = \rho^2 \, N_i^5(1, m_b, m_c) - \left. \frac{dN_i^5(\omega, m_b, m_c)}{d\omega} \right|_{\omega=1} . \tag{64}$$

decay	ω	N_1	N_2	N_3	N_1^5	N_2^5	N_3^5
	1.0	$1.28\ ^{+6}_{-6}$	$-0.19\ ^{+4}_{-4}$	$-0.06\ ^{+2}_{-1}$	0.99	$-0.24\ ^{+5}_{-4}$	$0.09\ ^{+2}_{-2}$
$\Lambda_b \to$	1.1	$1.25\ ^{+6}_{-5}$	$-0.18\ ^{+4}_{-4}$	$-0.06\ ^{+1}_{-1}$	0.97	$-0.23\ ^{+5}_{-4}$	$0.08\ ^{+2}_{-2}$
Λ_c	1.2	$1.21\ ^{+5}_{-5}$	$-0.17\ ^{+4}_{-3}$	$-0.05\ ^{+1}_{-1}$	0.95	$-0.21\ ^{+4}_{-4}$	$0.08\ ^{+2}_{-2}$
	1.3	$1.15\ ^{+5}_{-5}$	$-0.16\ ^{+4}_{-3}$	$-0.05\ ^{+1}_{-1}$	0.91	$-0.19\ ^{+4}_{-3}$	$0.07\ ^{+1}_{-1}$
	1.0	$1.32\ ^{+5}_{-6}$	$-0.23\ ^{+4}_{-4}$	$-0.07\ ^{+1}_{-1}$	0.99	$-0.28\ ^{+5}_{-4}$	$0.10\ ^{+2}_{-2}$
$\Xi_b \to$	1.1	$1.30\ ^{+5}_{-6}$	$-0.22\ ^{+4}_{-4}$	$-0.07\ ^{+1}_{-1}$	0.97	$-0.26\ ^{+5}_{-4}$	$0.10\ ^{+2}_{-2}$
Ξ_c	1.2	$1.26\ ^{+5}_{-5}$	$-0.20\ ^{+4}_{-3}$	$-0.06\ ^{+1}_{-1}$	0.95	$-0.24\ ^{+4}_{-4}$	$0.09\ ^{+1}_{-2}$
	1.3	$1.19\ ^{+4}_{-5}$	$-0.18\ ^{+4}_{-3}$	$-0.06\ ^{+1}_{-1}$	0.91	$-0.22\ ^{+4}_{-3}$	$0.08\ ^{+1}_{-1}$

Table 17: *Correction factors needed to relate the form factors at the physical limit with the Isgur-Wise function.*

decay	$-$	F_1	F_2	F_3	G_1	G_2	G_3
$\Lambda_c \to \Lambda_c$	$\tilde{\rho}$	$1.8\ ^{+0.9}_{-1.5}$	$-0.4\ ^{+2}_{-1}$	$-0.10\ ^{+7}_{-4}$	$1.3\ ^{+0.8}_{-1.2}$	$-0.4\ ^{+3}_{-2}$	$0.16\ ^{+\ 6}_{-10}$
$\Xi_c \to \Xi_c$	$\tilde{\rho}$	$2.3\ ^{+0.9}_{-1.4}$	$-0.5\ ^{+2}_{-2}$	$-0.15\ ^{+7}_{-4}$	$1.6\ ^{+0.6}_{-1.0}$	$-0.6\ ^{+3}_{-2}$	$0.22\ ^{+\ 7}_{-10}$

Table 18: *Slope of the physical form factors near zero recoil.*

Our results for $\tilde{\rho}_i^{V,A}$ are presented in Table 18. We observe that this procedure has the effect of taking us back to the form factors for physical $b \to c$ decays from the Isgur-Wise function, which, in turn, was determined by dividing the lattice data for the form factors (for unphysical quark masses) by the coefficients $N_i^{(5)}$. Clearly, most of the uncertainty in the factors $N_i^{(5)}$, due to their dependence on $\bar{\Lambda}$ and the quark masses, is now cancelled, as it should be for any physical quantity. To quantify this statement, we report the result of the following exercise. We have measured the ratio of the slopes of the form factor $G_1(\omega)$, at the chiral limit, letting $\bar{\Lambda}$ vary from 200 to 600 MeV, and changing the coefficients $N_i^{(5)}$ accordingly. We obtain

$$\frac{\tilde{\rho}_1^A(\bar{\Lambda}=200)}{\tilde{\rho}_1^A(\bar{\Lambda}=600)} = 1.00\ ^{+12}_{-\ 8}\,, \tag{65}$$

where the relatively large error is largely due to the extrapolation to the chiral limit.

6.2 Decay rates

Following Refs. [23] and [24], we define the helicity amplitudes, in terms of the physical form factors (61), in the velocity basis:

$$\begin{aligned} H^{V,A}_{\frac{1}{2},0} &= \frac{\sqrt{2M_{\Lambda_b}M_{\Lambda_c}(\omega \mp 1)}}{\sqrt{M^2_{\Lambda_b} + M^2_{\Lambda_c} - 2M_{\Lambda_b}M_{\Lambda_c}\omega}} \times \\ &\times \left((M_{\Lambda_b} \pm M_{\Lambda_c})F_1^{V,A} \pm M_{\Lambda_c}(\omega \pm 1)F_2^{V,A} \pm M_{\Lambda_b}(\omega \pm 1)F_3^{V,A}\right) \\ H^{V,A}_{\frac{1}{2},1} &= -2\sqrt{M_{\Lambda_b}M_{\Lambda_c}(\omega \mp 1)}F_1^{V,A} \end{aligned} \tag{66}$$

where, for brevity, we set

$$F_i^V = F_i(\omega), \qquad F_i^A = G_i(\omega). \tag{67}$$

and where the upper sign corresponds to V and the lower one to A.

The helicity amplitudes $H^{V,A}_{\lambda_c,\lambda_W}$ carry information about the helicity of the current ($\lambda_W = 0$ for a longitudinally polarised W and $\lambda_W = \pm 1$ for transversely polarised one), and of the daughter baryon Λ_c ($\lambda_c = \pm 1/2$). The missing amplitudes can be computed by means of the relations

$$H^{V,A}_{-\lambda_c,-\lambda_W} = \pm H^{V,A}_{\lambda_c,\lambda_W}. \tag{68}$$

For convenience, we also define:

$$H_{\lambda_c,\lambda_W} = H^V_{\lambda_c,\lambda_W} + H^A_{\lambda_c,\lambda_W}\ . \tag{69}$$

Differential decay rates can then be evaluated:

$$\begin{aligned} \frac{d\Gamma_T}{d\omega} &= \frac{G_F^2}{(2\pi)^3}|V_{cb}|^2 \frac{q^2 M^2_{\Lambda_c}\sqrt{(\omega^2-1)}}{12M_{\Lambda_b}}\left(|H_{1/2,1}|^2 + |H_{-1/2,-1}|^2\right), \\ \frac{d\Gamma_L}{d\omega} &= \frac{G_F^2}{(2\pi)^3}|V_{cb}|^2 \frac{q^2 M^2_{\Lambda_c}\sqrt{(\omega^2-1)}}{12M_{\Lambda_b}}\left(|H_{1/2,0}|^2 + |H_{-1/2,0}|^2\right), \end{aligned} \tag{70}$$

where Γ_T and Γ_L are the contributions to the rate from transversely and longitudinally polarised W's respectively, and whose sum is

$$\begin{aligned} \frac{d\Gamma}{d\omega} &= \frac{G_F^2}{(2\pi)^3}|V_{cb}|^2 \frac{q^2 M^2_{\Lambda_c}\sqrt{(\omega^2-1)}}{12M_{\Lambda_b}} \\ &\times \left(|H_{1/2,1}|^2 + |H_{-1/2,-1}|^2 + |H_{1/2,0}|^2 + |H_{-1/2,0}|^2\right)\ . \end{aligned} \tag{71}$$

As can be seen from Eqs. (70) and (71), these quantities can be estimated, near zero recoil, using our results for the form factors, in a model-independent way.

In complete analogy with what is done for $\bar{B} \to D^{(*)}\ell\bar{\nu}$ decays, we define a form factor, $\mathcal{B}(\omega)$, which reduces, in the heavy-quark limit, to the Isgur-Wise function, $\xi^{\rm ren}(\omega)$, defined in Eq. (7). In terms of this form factor, the rate of Eq. (71) is:

$$\begin{aligned}\frac{d\Gamma}{d\omega} &= \frac{G_F^2}{4\pi^3}|V_{cb}|^2 M_{\Lambda_c}^3 (M_{\Lambda_b} - M_{\Lambda_c})^2 \sqrt{\omega^2-1} \\ &\times \left(\frac{\omega+1}{2}\right) \frac{1+r^2-2r(2\omega+1)/3}{(1-r)^2} \\ &\times \left(1 + \left(\frac{\omega-1}{\omega+1}\right) \frac{1+r^2-2r(2\omega-1)/3}{1+r^2-2r(2\omega+1)/3}\right) |\mathcal{B}(\omega)|^2 \ , \end{aligned} \tag{72}$$

with $r = M_{\Lambda_c}/M_{\Lambda_b}$. Near $\omega = 1$, the form factor can be expanded as

$$\mathcal{B}(\omega) = G_1(1) \left\{ 1 - \rho_{\mathcal{B}}^2 \, (\omega - 1) + \mathcal{O}\left((\omega-1)^2\right) \right\} \tag{73}$$

and the results of Tables 17 and 18 can be used to determine $G_1(1)$ and $\rho_{\mathcal{B}}^2$. We find, combining errors in quadrature, a slope

$$\rho_{\mathcal{B}}^2 = 1.1 \pm 1.0 \tag{74}$$

for $\Lambda_b \to \Lambda_c \ell \bar{\nu}$ decays and

$$\rho_{\mathcal{B}}^2 = 1.4 \pm 0.8 \tag{75}$$

for $\Xi_b \to \Xi_c \ell \bar{\nu}$ decays. These values are the ones that should be compared to the slopes obtained by performing fits to experimental results for $d\Gamma/d\omega$ versus ω, for ω near 1, when such results become available. The results of Eqs. (74) and (75) can also be compared to the slopes we found for the corresponding Isgur-Wise functions (Eqs. (49) and (50)). These two sets of slopes are virtually indistinguishable, especially given the size of our present errors.

For both decays we find $G_1(1) = 0.99$ which is just $1 + \delta_1^5(1)\alpha_s$, as it should be at the level of precision at which we are working (see Eqs. (8) and (14)). In principle, though, $G_1(1)$ receives also $1/m_Q^2$ corrections and higher-order perturbative corrections, both of which are beyond the precision reached in the present paper.

We now turn to integrated rates. The physical limit for ω extends up to $\omega \simeq 1.43$, which is beyond the range of velocity transfer accessible to us ($\omega \in [1.0, 1.2]$) in the present simulation. We thus define the partially-integrated decay rate,

$$\Gamma_i^{\rm part}(\omega_{\rm max}) = \int_1^{\omega_{\rm max}} d\omega \, \frac{d\Gamma_i}{d\omega} \tag{76}$$

as a function of the upper limit of integration, for each of the rates $i = T, L$ and $T + L$.

In Table 19, we present our results for the quantities $\Gamma_i^{\rm part}(\omega_{\rm max})$ for several values of $\omega_{\rm max}$. For the case of the Λ_c, the Λ_b and the Ξ_c we have used the experimental

decay	$\omega_{\rm max}$	1.1	1.15	1.20	1.25	1.30
$\Lambda_b \to \Lambda_c$	$\Gamma^{\rm part}$	$0.57\ ^{+9}_{-7}$	$0.98\ ^{+25}_{-18}$	$1.4\ ^{+5}_{-4}$	$1.8\ ^{+\ 9}_{-\ 7}$	$2.2\ ^{+1.4}_{-1.2}$
$\Xi_b \to \Xi_c$	$\omega_{\rm max}$	1.1	1.15	1.20	1.25	1.30
	$\Gamma^{\rm part}$	$0.66\ ^{+7}_{-8}$	$1.1\ ^{+2}_{-2}$	$1.6\ ^{+4}_{-5}$	$1.9\ ^{+7}_{-8}$	$2.2\ ^{+1.2}_{-1.3}$
decay	$\omega_{\rm max}$	1.1	1.15	1.20	1.25	1.30
$\Lambda_b \to \Lambda_c$	$\Gamma_L^{\rm part}$	$0.23\ ^{+3}_{-2}$	$0.44\ ^{+8}_{-6}$	$0.71\ ^{+17}_{-13}$	$1.0\ ^{+3}_{-2}$	$1.4\ ^{+5}_{-4}$
$\Xi_b \to \Xi_c$	$\omega_{\rm max}$	1.1	1.15	1.20	1.25	1.30
	$\Gamma_L^{\rm part}$	$0.28\ ^{+2}_{-3}$	$0.54\ ^{+7}_{-8}$	$0.86\ ^{+14}_{-16}$	$1.2\ ^{+2}_{-3}$	$1.7\ ^{+4}_{-4}$
decay	$\omega_{\rm max}$	1.1	1.15	1.20	1.25	1.30
$\Lambda_b \to \Lambda_c$	$\Gamma_T^{\rm part}$	$0.34\ ^{+6}_{-4}$	$0.53\ ^{+16}_{-14}$	$0.7\ ^{+3}_{-3}$	$0.8\ ^{+6}_{-5}$	-
$\Xi_b \to \Xi_c$	$\omega_{\rm max}$	1.1	1.15	1.20	1.25	1.30
	$\Gamma_T^{\rm part}$	$0.38\ ^{+5}_{-5}$	$0.58\ ^{+13}_{-15}$	$0.7\ ^{+3}_{-3}$	-	-

Table 19: *Partial decay rates, in units of* $|V_{cb}|^2\ 10^{13}\ s^{-1}$, *for the* Λ *and* Ξ *semileptonic decays for various values of* $\omega_{\rm max}$. *The transverse decay rate is very sensitive to quadratic terms in* $(\omega - 1)$, *and the predictions for* $\omega > 1.2$ *are no longer reliable.*

values for the masses, whereas, for the Ξ_b, which is as yet undiscovered, we have used the value computed in our previous paper on heavy baryon spectroscopy [3]:

$$M_{\Xi_c} = 2.47 \text{ GeV [Exp]} \qquad M_{\Xi_b} = 5.76 \text{ GeV} \qquad \text{[Latt]}. \tag{77}$$

At present, a direct comparison of our results with experiments is not possible. Although the semileptonic decay of Λ_b has been observed by various experiments [2], a measurement of the decay rate is not yet available. The problem of determining the rate of the Λ_b and Ξ_b semileptonic decays has been addressed theoretically, making use of different models and approaches (e.g. infinite momentum frame (IMF), dipole form factors in Ref. [23] and quark model in Ref. [24]), by several authors. Their predictions for the rate, integrated up to the end-point, are reported in Figure 8, and compared with the function $\Gamma(\omega_{\rm max})$. To evaluate this function we have assumed $|V_{cb}| = 0.044$.

Finally, we note that many other interesting quantities could be computed and confronted with future experiments, e.g. asymmetry parameters (see for example [25]) and the ratio of the longitudinal to transverse rates. However, all these quantities are sensitive to either $1/m_Q^2$ effects or to terms proportional to $(\omega-1)^2$. Both of these effects are beyond the precision reached in the present study.

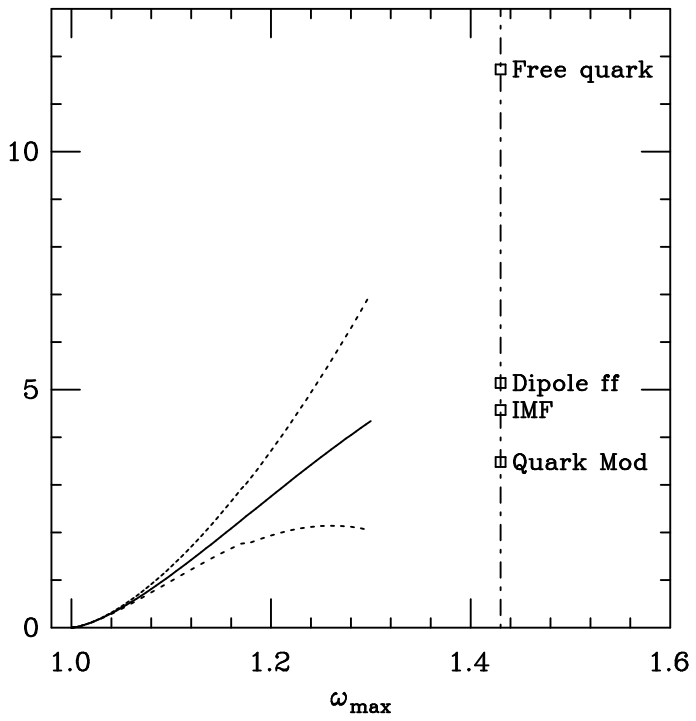

Figure 8: *Partially-integrated decay rate for the process* $\Lambda_b \to \Lambda_c + l\bar{\nu}$*, in units of* $10^{10}\, s^{-1}$*, as a function of the limit of integration* $\omega_{\rm max}$*. A comparison with several model estimates is shown at the end-point [23, 24]. The solid curve corresponds to our central values for* $\tilde{\rho}$ *and the dotted curves to the errors on these values.*

Conclusions

During the past few years lattice simulations have been applied very successfully to weak decays of heavy mesons, and in this work we have extended these techniques to heavy baryons. We have presented an extensive lattice study of the semileptonic $\Lambda_b \to \Lambda_c + l\bar{\nu}$ and $\Xi_b \to \Xi_c + l\bar{\nu}$ decays, resulting in predictions for the decay rates, for values of the velocity transfer up to about $\omega = 1.2$. We have developed the formalism necessary for extracting the decay amplitudes, demonstrated the feasibility of obtaining phenomenologically interesting results, and presented the first set of predictions. We anticipate that the application of lattice QCD to studies of the forthcoming experimental data on heavy-baryon decays will be an active area of phenomenology during the coming years.

HQET is an important tool in the application of lattice QCD to weak decays of heavy baryons, as it is also for mesons. In order to keep lattice artefacts reasonably small, we are forced to perform the computations with heavy quarks with masses not much larger than that of the charm quark, and then to extrapolate the results to physical $b \to c$ decays. HQET provides us with a sound theoretical formalism for performing this extrapolation.

Perhaps the weakest feature of our study was the inability to determine the behaviour of the decay amplitudes with the mass of the light quarks with sufficient precision. We did perform the computations for three combinations of masses for the two light quarks, which allowed us to attempt an extrapolation to the physical Λ (with two almost massless valence quarks) and Ξ (with one strange and one almost massless quark) baryons. However, in performing these extrapolations the statistical errors are amplified, and one of the priorities of a future simulation should be to generate substantial datasets for a larger set of light-quark masses. For example, it will be very interesting to check whether the slope of the Isgur-Wise function decreases as the masses of the light quarks are reduced, as expected theoretically. In the present simulation we have a hint that this is the case, but the statistical errors are too large to draw a definitive conclusion.

Acknowledgements

We are indebted to the staff of Edinburgh Parallel Computing Centre for the provision of services on the Meiko Computing Surface and on the Cray T3D. LL and JN thank the Theory Group in Southampton for its kind hospitality during the early stages of this project. This research was supported by the UK Science and Engineering Research Council under grant GR/G 32779, by the Particle Physics and Astronomy Research Council under grant GR/J 21347 and by the Engineering and Physical Sciences Research Council under grant GR/K 41663. CTS and

DGR acknowledge the Particle Physics and Astronomy Research Council for its support through the award of a Senior Fellowship and an Advanced Fellowship respectively. JN acknowledges support from DGES under contract PB95-1204. OO is supported by JNICT under grant BD/2714/93. We also acknowledge partial support by the EU contracts CHRX-CT92-0051 and ERBCHBICT-930877.

A The use of extended interpolating operators

In order to enhance the signal for the baryonic correlation functions, the light and heavy quark propagators have been computed using the Jacobi smearing method [12]. Since smearing is not a Lorentz-invariant operation, it alters the transformation properties of the correlation functions, particularly at non-zero momentum. In this Appendix we present the formalism required to extract the form factors from two- and three-point correlation functions computed using extended (smeared) interpolating operators for the baryons.

Consider the local operator $\mathcal{O}(x)$ defined in Eq. (24),

$$\mathcal{O}_\rho(x) = \epsilon_{abc} \Big(l_1^{aT}(x) \mathcal{C}\gamma_5 l_2^b(x) \Big) Q_\rho^c(x) \ , \tag{78}$$

where ρ is a spinor index. Here we have suppressed the index Q in labelling the operator. $\mathcal{O}$ has non-zero overlap with spin 1/2 states, such the $\Lambda-$baryon:

$$\langle 0|\mathcal{O}_\rho(0)|\vec{p},r\rangle = Z u_\rho^{(r)}(\vec{p}). \tag{79}$$

where r is the polarisation index.[5] The ket in Eq. (79) represents a heavy Λ state (e.g. Λ_b or Λ_c). The amplitude Z is a Lorentz scalar.

The smeared baryonic operator can be written as

$$\begin{aligned} \mathcal{O}_\rho^s(\vec{x},t) &= \epsilon_{abc} \sum_{\vec{y},\vec{z},\vec{w}} f(|\vec{y}-\vec{x}|) f(|\vec{z}-\vec{x}|) f(|\vec{w}-\vec{x}|) \times \\ &\times \Big(l_1^{aT}(\vec{y},t) \mathcal{C}\gamma_5 \, l_2^b(\vec{z},t) \Big) Q_\rho^c(\vec{w},t) \ . \end{aligned} \tag{80}$$

Because the smearing is performed only in the spatial directions, Lorentz symmetry is lost and only spatial translations, rotations, parity and time reversal survive. Therefore, the overlap of the operator $\mathcal{O}_\rho^s(\vec{x},t)$ with the state $|\vec{p},r\rangle$ is given by the more general expression

$$\begin{aligned} \langle 0|\mathcal{O}_\rho^s(0)|\vec{p},r\rangle &= \Big[\Big(Z_1(|\vec{p}|) + Z_2(|\vec{p}|)\gamma_0 \Big) u^{(r)}(\vec{p}) \Big]_\rho \\ \langle 0|\overline{\mathcal{O}}_\rho^s(0)|\vec{p},r\rangle &= \Big[\bar{v}^{(r)}(\vec{p}) \Big(Z_1(|\vec{p}|) - Z_2(|\vec{p}|)\gamma_0 \Big) \Big]_\rho \end{aligned} \tag{81}$$

where the amplitudes Z_1 and Z_2 may depend on the magnitude of the three-momentum of the state $|\vec{p},r\rangle$, in accord with the restricted symmetries of the system.

[5] Our spinors are normalized such that $u^{(r)\dagger}u^{(s)} = v^{(r)\dagger}v^{(s)} = (E/m)\,\delta^{rs}$.

A.1 Smeared two-point functions

We now study the consequences of the above discussion in the case of smeared source and sink (SS) two-point functions. Using Eq. (81), we can derive the general expression for the two-point function at large values of t and $(T-t)$ [6]

$$
\begin{aligned}
G^{SS}_{\rho\sigma}(t,\vec{p}) &= \sum_{\vec{x}} e^{-i\vec{p}\cdot\vec{x}} \langle \mathcal{O}_\rho(\vec{x},t)\bar{\mathcal{O}}_\sigma(\vec{0},0)\rangle \qquad (82)\\
&= \sum_{|\vec{q},r\rangle}\sum_{\vec{x}} \frac{m}{E(\vec{q})} e^{-i\vec{p}\cdot\vec{x}} \Big[e^{-E(\vec{q})t+i\vec{q}\cdot\vec{x}} \langle 0|\mathcal{O}_\rho(\vec{0},0)|\vec{q},r\rangle\langle\vec{q},r|\overline{\mathcal{O}}_\sigma(\vec{0},0)|0\rangle - \\
&\qquad - e^{-E(\vec{q})(T-t)-i\vec{q}\cdot\vec{x}}\ \langle 0|\overline{\mathcal{O}}_\sigma(\vec{0},0)|\vec{q},r\rangle\langle\vec{q},r|\mathcal{O}_\rho(\vec{0},0)|0\rangle\Big] \\
&= \sum_r \frac{m}{E(\vec{p})} \Big\{ \Big[e^{-E(\vec{p})t}\Big(Z_1(|\vec{p}|) + Z_2(|\vec{p}|)\gamma_0\Big) u^{(r)}(\vec{p})\ \times \\
&\qquad \times\ \bar{u}^{(r)}(\vec{p})\Big(Z_1(|\vec{p}|) + Z_2(|\vec{p}|)\gamma_0\Big)\Big]_{\rho\sigma} \\
&\qquad - \Big[e^{-E(\vec{p})(T-t)}\Big(Z_1(|\vec{p}|) - Z_2(|\vec{p}|)\gamma_0\Big) v^{(r)}(-\vec{p})\ \times \\
&\qquad \times\ \bar{v}^{(r)}(-\vec{p})\Big(Z_1(|\vec{p}|) - Z_2(|\vec{p}|)\gamma_0\Big)\Big]_{\rho\sigma} \Big\}\ .
\end{aligned}
$$

We find it convenient to write the spin matrix $G^{SS}_{\rho\sigma}$ in terms of the parameters

$$
Z_s = Z_1 + Z_2, \qquad \alpha = (Z_1 - Z_2)/(Z_1 + Z_2)\ : \qquad (83)
$$

rather than Z_1 and Z_2:

$$
\begin{aligned}
G^{ss}_{\rho\sigma}(t,\vec{p}) \;=\; & Z_s^2(|\vec{p}|) e^{-E(\vec{p})t} \left\{ \left[\frac{E+m-\alpha^2(E-m)}{4E}\mathbb{1} + \right.\right. \qquad (84)\\
& \left.\left. + \frac{E+m+\alpha^2(E-m)}{4E}\gamma_0 - \frac{2\alpha}{4E}\vec{p}\cdot\vec{\gamma}\right] \right. \\
- \;& e^{-E(\vec{p})(T-t)} \left[\frac{E+m-\alpha^2(E-m)}{4E}\mathbb{1} - \right. \\
& \left.\left. - \frac{E+m+\alpha^2(E-m)}{4E}\gamma_0 - \frac{2\alpha}{4E}\vec{p}\cdot\vec{\gamma}\right] \right\}.
\end{aligned}
$$

Local operators, and full 4-dimensional cubic symmetry, correspond to the case $\alpha = 1$, i.e. $Z_2 = 0$.

A.2 Smeared three-point functions for the study of the semileptonic decay of the Λ_b.

We now present the expressions for the smeared-smeared three-point functions from which the form factors are extracted. The $V-A$ weak current J_μ is of course

[6] Note that we are using anti-periodic boundary conditions in time.

a local operator; it is the interpolating operators for the baryons in Eq. (23) which are now smeared. In the forward half of the lattice (F), for large t, so that only the lightest state contributes, we obtain

$$\begin{aligned} C^F(t_x,t_y) &= K(t_x,t_y)\Big\{\Big[E+M+\alpha(M-E)\Big]\mathbb{1}+ \\ &\quad +\Big[E+M-\alpha(M-E)\Big]\gamma_0+\Big[(1-\alpha)\vec{p}\cdot\vec{\gamma}\gamma_0\Big]- \\ &\quad -\Big[(1+\alpha)\vec{p}\cdot\vec{\gamma}\Big]\Big\}\times \\ &\times \Big\{\Big[F_1^L(\omega)\gamma_\mu+F_2^L(\omega)v'_\mu+F_3^L(\omega)v_\mu\Big]- \\ &\quad -\Big[\Big(G_1^L(\omega)\gamma_\mu+G_2^L(\omega)v'_\mu+G_3^L(\omega)v_\mu\Big)\gamma_5\Big]\Big\}\times \\ &\times \Big\{\Big[E'+M'+\beta(M'-E')\Big]\mathbb{1}+\Big[E'+M'-\beta(M'-E')\Big]\gamma_0- \\ &\quad -\Big[(1-\beta)\vec{p'}\cdot\vec{\gamma}\gamma_0\Big]-\Big[(1+\beta)\vec{p'}\cdot\vec{\gamma}\Big]\Big\} \end{aligned} \tag{85}$$

whereas in the backward half (B), for large $T-t$,

$$\begin{aligned} C^B(t_x,t_y) &= K(T-t_x,T-t_y)\Big\{\Big[E+M+\alpha(M-E)\Big]\mathbb{1}- \\ &\quad +\Big[E+M-\alpha(M-E)\Big]\gamma_0-\Big[(1-\alpha)\vec{p}\cdot\vec{\gamma}\gamma_0\Big]- \\ &\quad -\Big[(1+\alpha)\vec{p}\cdot\vec{\gamma}\Big]\Big\}\times \\ &\times \Big\{\Big[F_1^L(\omega)\gamma_\mu-F_2^L(\omega)\tilde{v}'_\mu-F_3^L(\omega)\tilde{v}_\mu\Big]+ \\ &\quad +\Big[\Big(G_1^L(\omega)\gamma_\mu+G_2^L(\omega)\tilde{v}'_\mu+G_3^L(\omega)\tilde{v}_\mu\Big)\gamma_5\Big]\Big\}\times \\ &\times \Big\{\Big[E'+M'+\beta(M'-E')\Big]\mathbb{1}-\Big[E'+M'-\beta(M'-E')\Big]\gamma_0+ \\ &\quad +\Big[(1-\beta)\vec{p'}\cdot\vec{\gamma}\gamma_0\Big]-\Big[(1+\beta)\vec{p'}\cdot\vec{\gamma}\Big]\Big\} \end{aligned} \tag{86}$$

where $\tilde{v}\equiv(E,-\vec{p})/M$ (similarly for $\tilde{v}'$) and where in both these equations the normalisation factor is given by:

$$K(t_x,t_y)=\frac{Z_sZ'_s}{16EE'}e^{-E(t_x-t_y)}e^{-E't_y}. \tag{87}$$

Since $t_x=24=T/2$ in our simulations, the dependence on t_x is the same in both halves of the lattice. In Eqs. (85) and (86) α and β are the functions defined in (83), for the final and initial particle respectively. They are identical only for degenerate transitions when $|\vec{p}|=|\vec{p'}|$. For local operators, $\alpha=\beta=1$ and expressions (85-86) reduce to Eq. (27).

Expressions (85) and (86) are used in Section 4 to extract the values of the form factors from the correlation functions. Further clarification of the procedures which are used is pressented in the following appendix.

B On the analysis of three-point correlators

In this appendix we discuss in greater detail the analysis procedure used to extract the six form factors from the correlation functions. Such an analysis is complicated both by the very large number of non-vanishing components of the three-point correlation function, which has both spinorial and Lorentz indices, and by the effect of the smearing on the baryonic operators discussed in the previous appendix. It proved to be convenient to restrict the analysis to those components which are proportional to large, and hence precisely measured, kinematical coefficients, as we now explain.

For illustration we consider here the forward half of the lattice; the extension to the backward half is straightforward. We consider two typical cases.

- **Example 1**: Coefficient of the form factor F_1^L for $\mu = 0$.

  We rewrite the expression in Eq. (85), which is a 4×4 matrix in spinor space, in terms of 2×2 matrices [7]:

$$\begin{aligned}
\frac{\text{Vector}_0}{K(t_x,t_y)} &= 4\left[(E+M)(E'+M') + \vec{p}\cdot\vec{p}\,'\right](\mathbb{1}+\gamma_0) \\
&+ 4\alpha\beta\left[-(E-M)(E'-M') - \vec{p}\cdot\vec{p}\,'\right](\mathbb{1}-\gamma_0) \\
&+ 4ip_ip'_j\sigma^{ij}(\mathbb{1}+\gamma_0) - 4\alpha\beta ip_ip'_j\sigma^{ij}(\mathbb{1}-\gamma_0) \\
&+ 4\alpha\left[(M-E)p_i - (E'+M')p_i\right]\gamma_i(\mathbb{1}+\gamma_0) \\
&- 4\beta\left[(M+E)p_i - (E'-M')p_i\right]\gamma_i(\mathbb{1}-\gamma_0), \qquad (89)
\end{aligned}$$

  where Vector_0 denotes the time component of the three point correlation function with the vector current. So the matrix structure shared by the coefficients of the vector form factors is of the form:

$$\frac{\text{Vector}_0}{K(t_x,t_y)} \propto \begin{pmatrix} \begin{pmatrix} 1 & \\ & \end{pmatrix} & \begin{pmatrix} \beta & \\ & \end{pmatrix} \\ \begin{pmatrix} \alpha & \\ & \end{pmatrix} & \begin{pmatrix} \alpha\beta & \\ & \end{pmatrix} \end{pmatrix} \qquad (90)$$

  where each of the submatrices is a 2×2 matrix.

[7] The following representation for the gamma matrices is used here:

$$\gamma_0 = \begin{pmatrix} 1 & 0 \\ 0 & -1 \end{pmatrix}; \quad \gamma_i = \begin{pmatrix} 0 & \sigma_i \\ -\sigma_i & 0 \end{pmatrix} \text{ with } i = 1,2,3. \qquad (88)$$

- **Example 2**: Coefficient of the form factor G_1^L for $\mu = k = 1, 2, 3$.
  A similar manipulation of Eqs. (85) for the axial current leads to

$$\begin{aligned}\frac{\text{Axial}_k}{K(t_x,t_y)} &= \Big\{4\left[(M+E)(M'+E')\right]\gamma_k(\mathbb{1}+\gamma_0) \\ &+ 4\alpha\beta\left[(M-E)(M'-E')\right]\gamma_k(\mathbb{1}-\gamma_0) \\ &+ 4\alpha\left[(M-E)p'_i\gamma_k\gamma_i - (M'+E')p_i\gamma_i\gamma_k\right](\mathbb{1}+\gamma_0) \\ &+ 4\beta\left[(M+E)p'_i\gamma_k\gamma_i + (E'-M')p_i\gamma_i\gamma_k\right](\mathbb{1}-\gamma_0) \\ &+ 4\left[p_ip'_j\gamma_i\gamma_k\gamma_j\right](\mathbb{1}+\gamma_0) + 4\alpha\beta\left[p_ip'_j\gamma_i\gamma_k\gamma_j\right](\mathbb{1}-\gamma_0)\Big\}\gamma_5\ ,\end{aligned} \tag{91}$$

  which also has the structure of (90).

The relative sizes of the components of the matrices (89) and (91) are as follows:

- the submatrices proportional to the identity are proportional to MM' (plus small terms quadratic in the momenta), and are therefore *large* and precisely determined.
- the submatrices proportional to α and β are proportional to terms like Mp'_i or $M'p_i$ and are therefore *medium*-sized. Furthermore they have an additional statistical uncertainty due to the presence of the amplitude factors α or β.
- the submatrices proportional to $\alpha\beta$ are proportional to $(E'-M')(E-M)$ or other terms which are quadratic in the momenta, and are therefore *small*.

Finally, we note that, as a general feature, the vector current will give large contributions for $\mu = 0$ and the axial current when $\mu = i$, $i = 1, 2, 3$.

C Determination of Z_V

In this appendix we discuss the normalisation of the lattice vector current, used for extracting the vector form factors. The normalisation factor, Z_V has previously been determined from matrix elements between heavy meson states, using the same configurations, and for the same values of the quark masses as those used in the present study [21], and we present the results below. We start however with a determination of Z_V from matrix elements between heavy baryon states.

Z_V can be measured from the correlators (23), computed for degenerate initial and final heavy quarks ($Q = Q'$). For instance, with Dirac index $i = 1, 2$, we define

$$Z_V(t) = \mathcal{K}\frac{\left[C_2^Q(\vec{p}, T/2)\right]_{ii}}{\left[C(\vec{p}, \vec{q}=\vec{0}, T/2, t)_{\mu=0}^{Q\to Q}\right]_{ii}} = \frac{1}{F_1^L(1) + F_2^L(1) + F_3^L(1)} \tag{92}$$

with

$$\mathcal{K} = \frac{(E+M)}{2E} \frac{2E}{E+M-\alpha^2(M-E)} \tag{93}$$

and where C_2^Q was defined in Eq. (31) and t is taken in $(0, T/2)$. Z_V is then obtained by fitting $Z_V(t)$ to a constant in the plateau region.

We have computed the necessary two- and three-point correlators for two different forward channels: $\vec{p} = \vec{0}$ and $\vec{p} = (p_{\min}, 0, 0)$. From the correlation functions with the baryon at rest we obtain:

$$\begin{array}{rcll} Z_V &=& 0.898\ ^{+3}_{-2} & \text{at} \quad \kappa_{l1} = \kappa_{l2} = 0.14144,\ \kappa_Q = 0.133 \\ Z_V &=& 0.924\ ^{+2}_{-2} & \text{at} \quad \kappa_{l1} = \kappa_{l2} = 0.14144,\ \kappa_Q = 0.129 \\ Z_V &=& 0.948\ ^{+2}_{-2} & \text{at} \quad \kappa_{l1} = \kappa_{l2} = 0.14144,\ \kappa_Q = 0.125 \\ Z_V &=& 0.970\ ^{+1}_{-2} & \text{at} \quad \kappa_{l1} = \kappa_{l2} = 0.14144,\ \kappa_Q = 0.121 \end{array} . \tag{94}$$

The statistical errors are very small (although not as small as for meson states), which is not unexpected since we are studying the effects of the charge operator.

For Z_V measured from correlation functions with $\vec{p} = (p_{\min}, 0, 0)$, the statistical errors are too large for us to make any comparison with the results in (94). In this case we find:

$$\begin{array}{rcll} Z_V &=& 0.88\ ^{+15}_{-10} & \text{at} \quad \kappa_{l1} = \kappa_{l2} = 0.14144,\ \kappa_Q = 0.133 \\ Z_V &=& 0.90\ ^{+14}_{-11} & \text{at} \quad \kappa_{l1} = \kappa_{l2} = 0.14144,\ \kappa_Q = 0.129 \\ Z_V &=& 0.94\ ^{+14}_{-11} & \text{at} \quad \kappa_{l1} = \kappa_{l2} = 0.14144,\ \kappa_Q = 0.125 \\ Z_V &=& 0.97\ ^{+15}_{-12} & \text{at} \quad \kappa_{l1} = \kappa_{l2} = 0.14144,\ \kappa_Q = 0.121\ . \end{array} \tag{95}$$

We now compare the results for Z_V obtained between baryonic states (Eq. (94)), and those obtained in Ref. [21] from matrix elements between pseodoscalar states using the same configurations and quark masses:

$$\begin{array}{rcll} Z_V &=& 0.8913\ ^{+2}_{-1} & \text{at} \quad \kappa_l = 0.14144,\ \kappa_Q = 0.133 \\ Z_V &=& 0.9177\ ^{+3}_{-2} & \text{at} \quad \kappa_l = 0.14144,\ \kappa_Q = 0.129 \\ Z_V &=& 0.9428\ ^{+4}_{-2} & \text{at} \quad \kappa_l = 0.14144,\ \kappa_Q = 0.125 \\ Z_V &=& 0.9659\ ^{+6}_{-3} & \text{at} \quad \kappa_l = 0.14144,\ \kappa_Q = 0.121\ . \end{array} \tag{96}$$

The agreement of the results obtained for Z_V using mesonic and baryonic correlation functions to within less than 1% is reassuring.

The variation of the values of Z_V with the mass of the heavy quark in (94) and (96) is an effect of the discretisation errors, due to the fact that the quark Q is heavy. To see this more clearly we compare the results with those obtained

between light pseudoscalar mesons (with degenerate valence quarks):

$$\begin{aligned} Z_V &= 0.8314(4) \quad \text{at } \kappa = 0.14144 \\ Z_V &= 0.8245(4) \quad \text{at } \kappa = 0.14226 \\ Z_V &= 0.8214(6) \quad \text{at } \kappa = 0.14262 \ . \end{aligned} \tag{97}$$

The results in (97) were obtained on a subset of 10 gluon configurations [20]. The dependence on the masses of the light quarks is seen to be very mild, and the reuslts are in consistent with the expectations from one-loop perturbation theory [26]:

$$Z_V = 1 - 0.10g^2 + \mathcal{O}(g^4) \simeq 0.83 \text{ at } \beta = 6.2 \tag{98}$$

when evaluated using the boosted value of the coupling constant, obtained from the mean field resummation of tadpole diagrams[27].

The results for Z_V in Eq. (94) and (96), obtained using heavy baryon and meson states, differ from those obtained with light mesons, (97), by about 10-20% for the range of quark masses used in our simulations. This difference is a good indication of the size of mass-dependent discretisation errors in our calculation; it is consistent with our expectation that they should be of $\mathcal{O}\left(\alpha_s a m_Q\right)$ and $\mathcal{O}\left(a^2 m_Q^2\right)$. However, as explained in Section 4, the errors in the computed form factors are expected to be considerably smaller, because we normalise all of them by Z_V also determined between heavy baryon states.

References

[1] C. Albajar *et al.*, Phys. Lett. **B273**, (1991) 540;
G. Bari *et al.*, Nuovo Cimento **A104** (1991) 1787.

[2] ALEPH Collaboration, D. Decamp *et al.*, Phys. Lett. B **278**, 367 (1992);
OPAL Collaboration, P. Acton *et al.*, Phys. Lett. B **281**, 394 (1992);
ALEPH Collaboration, D. Buskulic. *et al.*, Phys. Lett. B **294**, 145 (1992);
DELPHI Collaboration, P. Abreu *et al.*, Phys. Lett. B **311**, 379 (1993).

[3] UKQCD Collaboration, K.C. Bowler *et al.*, Phys. Rev. D **54**, 3619 (1996).

[4] N. Isgur and M.B. Wise, Nucl. Phys. **B348**, 292 (1991);
H. Georgi, Nucl. Phys. **B348**, 293 (1991) ;
T. Mannel, W. Roberts and Z. Ryzak, Nucl. Phys. **B355**, 38 (1991);
F. Hussain *et al.*, Zeit. Phys. C **51**, 321 (1991) and Nucl. Phys. **B370**, 259 (1992).

[5] M. Neubert, Phys. Rept. **245**, 259 (1994).

[6] M. Neubert, Phys. Rev. D **46**, 2212 (1992).

[7] M.E. Luke, Phys. Lett. B **252**, 447 (1990).

[8] M. Crisafulli, V. Giménez, G. Martinelli and C.T. Sachrajda, Nucl. Phys. **B457**, 1995 (594).

[9] UKQCD Collaboration, C.R. Allton *et al.*, Nucl. Phys. **B407**, 331 (1993).

[10] B. Sheikholeslami and R. Wohlert, Nucl. Phys. **B259**, 572 (1985).

[11] G. Heatlie, C.T. Sachrajda, G. Martinelli, C. Pittori and G.C. Rossi, Nucl. Phys. **B352**, 266 (1991).

[12] UKQCD Collaboration, C.R. Allton *et al.*, Phys. Rev. D **47**, 5128 (1993).

[13] B. Efron, SIAM Review 21, 460 (1979).

[14] M. C. Chu, M. Lissia and J.W. Negele, Nucl. Phys. **B360**, 31 (1991).

[15] G. Martinelli, Nucl. Phys. B (Proc. Suppl.) **9**, 139 (1989).

[16] UKQCD Collaboration, L. Lellouch *et al.*, Nucl. Phys. **B444**, 401 (1995).

[17] P. Marenzoni, G. Martinelli and N. Stella, Nucl. Phys. **B455**, 339 (1995).

[18] R. Sommer, Nucl. Phys. **B411**, 839 (1994); G. de Divitiis *et al.*, Nucl. Phys. **B437**, 447 (1994) .

[19] E. Gabrielli *et al.*, Nucl. Phys. **B362**, 475 (1991).

[20] UKQCD Collaboration, D.S. Henty, R.D. Kenway, B.J. Pendleton and J.I. Skullerud, Phys. Rev. D **51**, 5323 (1995).

[21] UKQCD Collaboration, K.C. Bowler *et al.*, Phys. Rev. D **52**, 5067 (1995).

[22] G. Martinelli and C.T. Sachrajda, Nucl. Phys. **B478**, 660 (1996).

[23] J.G. Körner, M. Krämer and D. Pirjol, Prog. Part. Nucl. Phys. **33**, 787 (1994).

[24] M.A. Ivanov and V.E. Lyubovitskii, hep-ph/9502202.

[25] A.F. Falk and M. Neubert, Phys. Rev. D **47**, 2982 (1993).

[26] A. Borrelli, R. Frezzotti, E. Gabrielli and C. Pittori, Nucl. Phys. **B409**, 382 (1993).

[27] G.P. Lepage and P.B. Mackenzie, Phys. Rev. D **48**, 2250 (1993).